TALLINN UNIVERSITY OF TECHNOLOGY
School of Information Technologies

Mario Stepanov 163119IVEM

Lap Timing System for Formula Student Car FEST21

Master's thesis

Supervisor: Olev Märtens
PhD

Tallinn 2021

TALLINNA TEHNIKAÜLIKOOL
Infotehnoloogia teaduskond

Mario Stepanov 163119IVEM

Ajavõtusüsteem tudengivormelile FEST21

Magistritöö

Juhendaja: Olev Märtens

Doktorikraad

Tallinn 2021

Author's declaration of originality

I hereby certify that I am the sole author of this thesis. All the used materials, references to the literature and the work of others have been referred to. This thesis has not been presented for examination anywhere else.

Author: Mario Stepanov

09.05.2021

Abstract

In this thesis, a lap timing system was developed, which is also capable of split time measurement and outputting via CAN bus and digitally. The thesis defines the requirements for the end system and provides research of current similar devices on the market. Two possible concepts are proposed and theoretical background of necessary terms are explained. The main components are tested regarding different codings, maximum achievable transmit frequency and communication distance. The concept is chosen and theoretical accuracy calculated. The hardware is designed according to requirements and main component testing results. For beacon, power-efficiency was considered in design, as it runs on battery. Software architecture is described, implemented and some critical points visualized.

As there was no possibility to get a verification device with desired accuracy for verification, the verification was done with a device with same accuracy to provide at least basic acceptance. The designed system was proved to be close to what it was designed for.

This thesis is written in English and is 45 pages long, including 9 chapters, 41 figures and 6 tables.

Annotatsioon

Ajavõtusüsteem tudengivormelile FEST21

Antud töös arendati ajavõtusüsteem, mis suudab eristada nii ringi- kui ka vaheaegu. Süsteem väljastab vastava signaali nii CAN siinile kui ka digitaalselt mille tuvastab vormeli logimisseade. Selle peale arvutab logimisseade logis välja ringi -ja vaheajad, mis on mugavalt näha ka kõikidel graafikutel. See lihtsustab logide analüüsi ja kiirendab sellega vormeli testimisprotsessi.

Töö esimeses osas seati süsteemile nõuded nagu täpsus, patarei pealt töötamise aeg ja maksimaalne töötamise kaugus. Seepeale uuriti praeguseid turult saadaolevaid seadmeid, mida kasutatakse motospordis aja mõõtmiseks. Siis kirjeldati mõningaid teoreetilisi termineid, mida kasutati antud lõputöö raames. Pakuti välja 2 infrapuna majakas-vastuvõtjal põhinevat ajavõtusüsteemi kontseptsiooni, mille täpsuse ja töökindluse kriitilised kohad toodi välja. Samuti arvutati välja teoreetiline täpsuse viga, mis olid tingitud CAN siini, logimisseadme ja infrapuna koodi vastuvõtmise viidetest. Põhikomponente testiti veendumaks nende sobivuses lõpprakenduses. Testiti maksimaalset koodi saatmise sagedust, maksimaalset kommunikatsiooni vahemaad ja selle vastavust teoreetilisele arvutusele. Pärast edukat põhikomponentide testimist disainiti riistvara nii infrapuna saatjale kui ka vastuvõtjale. Infrapuna saatja asetatakse testimisel raja kõrvale, kus ta perioodiliselt saadab välja oma ringi- või vaheaja unikaalset koodi. See peab töötama patarei-toitelt, mistõttu oli selle disainis oluline ka energiasäästlikkus. Infrapuna vastuvõtja aga asetseb vormeli peal, saades sealt energiat et võtta vastu infrapuna saatjalt tulev kood ja edastada see signaal vormeli logimissüsteemi. Kirjeldati süsteemi tarkvaraline arhitektuur ja kriitlisemad osad näidati diagrammil.

Süsteemi valideerimiseks ei leitud soovitud täpsusega seadet, mis oleks piisav tagamaks seadme vastavus püstitatud nõuetele. Siiski valideeriti seade sama täpsusklassi seadme vastu, et olla kindel selle üldises usaldusväärsuses.

Lõputöö on kirjutatud inglise keeles ning sisaldab teksti 45 leheküljel, 9 peatükki, 41 joonist, 6 tabelit.

List of abbreviations and terms

AC	Alternating Current
ADC	Analog-to-Digital Converter
AGC	Automatic Gain Control
APB	Advanced Peripheral Bus
ARR	Auto Reload Register
ATC	Automatic Threshold Control
CAN	Controller Area Network
CCR	Capture/Compare Register
CNT	Counter register
DCDC	DC-to-DC converter
DIP	Dual In-line Package
EAL	*Eesti Autospordi Liit*
EMI	Electromagnetic Interference
FEST	Formula Estonia
FS Team Tallinn	Formula Student Team Tallinn
GLONASS	Global Navigation Satellite System
GPIO	General Purpose Input/Output
GPS	Global Positioning System
HAL	Hardware Abstraction Layer
IR	Infrared
LED	Light Emitting Diode
MCU	Microcontroller Unit
MOSFET	Metal–Oxide–Semiconductor Field-Effect Transistor
PCB	Printed Circuit Board
PCM	Pulse-Code Modulation
PSC	Prescaler register
PWM	Pulse-Width Modulation
RC	Radio Control

RFID   Radio-Frequency Identification

SI   *Système International*

SWD   Serial Wire Debug

TSSOP   Thin-Shrink Small-Outline Package

UART   Universal Asynchronous Receiver-Transmitter

UHF   Ultra High Frequency

Table of contents

List of figures

List of tables

1 Introduction

Formula student is and international design competition between student teams. The goal is to design and manufacture a single-seater race car with defined ruleset, with focus on safety. The race car design is evaluated during static and dynamic disciplines. Static disciplines include cost, design and business concept of the race car. In dynamic disciplines different driving characteristics are evaluated, such as acceleration, skid pad, autocross. In addition to combustion vehicles, electric and driverless categories are present [1].

FS Team Tallinn have competed in Formula Student competition since 2006, by designing a new race car every year. Starting with combustion vehicles and switching to electric race cars in 2013. Some previous electric vehicles have been converted to driverless and competed in the driverless category. To evaluate formula student race car performance in dynamic disciplines, a lap timing system is needed.

This master thesis focuses on design of lap timing system for FEST21 (Formula Estonia 21). The thesis consists of 7 chapters where "Requirements" gives overview of set targets for the system. "State-of-the-art" lists similar devices currently available. "Background" provides basic terms need to be understood designing this system. In "Design concept", different concepts are proposed and theoretical error is calculated. "Hardware" provides electronic schematics and reasoning for hardware design. "Software" describes architecture and approach used in software design. Finally, in "Verification" chapter the designed system results are compared to existing device.

2 Requirements

2.1 Problem statement

During testing phase of developing formula student car, lap times need to be measured. Lap time is the ultimate measure (in dynamic disciplines) to compare teams performance at competitions. So far, the FS Team Tallinn has been up to top teams in acceleration and skid pad events but mostly lacking speed in autocross event, where lap times are around a minute. In response to this problem, measuring split times is proposed to better locate the sections of time loss. That also quickens the analysis of testing different set-ups and enhances driver training.

Currently, infrared beacon and receiver technology is used from Motec. For every extra split time measurement, a beacon device must be added which in the end, in case of three to five split time measurements makes it too expensive for the team overall - additional 520 EUR for every split time [2].

The testing is mostly done on various kart tracks around Tallinn and some bigger parking lots with cones added to simulate a specific discipline. The tracks are narrow and curved and therefore the maximum speed the car is designed to is around 120 km/h.

The most demanding disciplines regarding the timing accuracy are acceleration and skid pad. For example, times of skid pad event from Formula Student Germany 2018 are seen in Table 1. The top 8 teams are within 113 milliseconds, which makes it a good example for proposing the demanded accuracy.

Table 1. Formula Student Germany 2018 Skid Pad results.

Team	Time(s)
München TU	4.814
Trondheim NTNU	4.822
Stuttgart DHBW	4.832
Delft TU	4.835
Stuttgart U	4.876
Barcelona UPC	4.882
Tallinn TU	4.923
Amberg OTH	4.927

Finally, the timing system must conform with the systems in the car and team requirements. That includes the output via CAN bus and digital output. The requirements are summed up in the following list:

- Must be possible to differ lap and split times between each other.
- Be able to capture lap and split times within the full track width (4 m) at the maximum speed of car – 120 km/h.
- Have at least 10 milliseconds accuracy.
- Whole system with 3 split times and lap times should cost less than 500 EUR.
- The setup must be quick and temporary.
- CAN bus and digital output capability within the car.
- Continuous working hours on battery 24 hours.

3 State-Of-The-Art

3.1 Technologies

There are number of different technologies used in motorsport. Each has its own advantages and disadvantages. For specific application, each option must be overlooked to find the best solution. Following is an overview of technologies used for lap timing in motorsport.

3.1.1 GPS

There are numerous GPS Lap Timers in the market. For hobbyists there are a lot of Android apps to choose from. GPS basically works everywhere, except underground and does not require additional setup. The main disadvantage is the low sampling rate (10 Hz) and therefore bad lap time accuracy (0.1 s). With better sampling rate, the prices also rise exponentially. Also, the device needs some minutes start-up time to find satellites. Newer models also feature GLONASS [3].

3.1.2 Magnetic strip

Magnetic strip timing consists of a permanent magnetic strip on a track and a magnetic field sensor in a car. Multiple strips can be set up in a way to catch split times as well. The timing is accurate, cheap and reliable. But it requires permanent setup and is therefore dependant on the track [3].

3.1.3 RFID

The system consists of a RFID (Radio-frequency identification) tag and RFID reader connected to antenna. RFID tag is placed on a vehicle, which drives past the RFID reader's antenna. Depending on the type of RFID - active or passive the detection is different. In case of passive RFID, the radio signal sent from the antenna is used to power on the RFID tag and reflect energy back to the reader, where it is detected. In case of active RFID, the RFID tag transmits their own signal. Transponders transmit their signal only when they are woken up by the signal from antenna, but beacons broadcast their signal continuously in certain period.

UHF (Ultra-high frequency) RFID has a range up to 6 meters. With battery powered active RFID tags, more than 30 meters of range can be achieved [4].

3.1.4 Laser beam – photocell

High-frequency infra-red signal is transmitted and received using a photoresistor. If the beam is interrupted and the signal is not received when transmitted, the lap time is detected. This technology is accurate (1/10000 s) and widely used in other sports besides motorsport. It is also used as a backup for a transponder-based timing systems [5].

3.1.5 Infrared beacon and receiver

Lap timing by infrared LED-s consists of a transmitter and receiver. Transmitter marks the start/finish line by flashing the IR LED in an unique combination, known to receiver. The receiver is located on the vehicle and contains an IR photodiode to detect the code sent from the transmitter. Lap and split times can be separated by the code. This system is also widely used in RC cars and drone racing, but other way round - transmitters on drones and receivers on ground [6]. In motorsports the combination of a receiver on the vehicle and transmitters on the ground are used. This method is relatively inexpensive, relatively accurate and widely applicable.

3.2 Market

There is a variety of different lap timing devices, with different accuracies and prices in market. The RFID-based and photocell systems are accurate, but the lap information is detected on the track, not on the racing car. The GPS-based systems are cost-effective, but too inaccurate for desired application. There are a lot of infrared beacon-based systems which are also cost-effective, with most of them with undefined accuracy. Some of them lack a CAN bus communication or split time capability. A subset of each category devices are listed in Table 2.

Table 2. Market research of lap timing devices

Number	Name	Technology	CAN bus	Accuracy (s)	Notes	Price
1	Motec BR2 + BTX	Infrared	Yes	Not defined	Split times	~800 EUR [7]
2	AIM IR Lap + split transmitter	Infrared		Not defined	Only digital output, split times	~200 EUR [8]
3	Stack ST544 + ST546	Infrared		1/100	Only digital output, no split times	~515 EUR [9]
4	Longacre 21710	Infrared		Not defined	No digital output, small display included	~260 EUR [10]
5	Tag Heuer WIRELESS PHOTOCELL HL3-131 + CHRONOPRINTER 545	Photocell		1/100000	Wireless output to the timer, 1/100,000 sec. accuracy	~2200 EUR [11]
6	Cronox 2.0	Photocell		1/1000	1/1000 seconds accuracy, Bluetooth	~225 EUR [12]
7	Vbox Lap Timer v2	GPS	Yes	1/10	Display included, 10Hz GPS	~850 EUR [13]
8	Conrad LT-Q6000	GPS		1/10	10Hz GPS, USB/Bluetooth connection	~415 EUR [14]
9	Westhold IDEC	RFID		1/10000	-	~3000 EUR [15]

4 Background

There are number of terms need to be understood for designing something based on infrared communication. Because the communication environment is not constant, unexpected noise sources can interfere the communication and make it impossible.

4.1 Steradian

Steradian is a SI (*Système International)* unit of solid angle. It describes two-dimensional spans in three-dimensional space. The unit is dimensionless because it corresponds to m^2/m^2. However, the symbol *sr* is still used to distinguish it from other dimensionless units. A steradian stands for solid angle subtended at the centre of a sphere of radius r by unit area on its surface A, which equals r^2 as shown in equation (1). It is visualized in Figure 1 [16].

$$\Omega = \frac{A}{r^2} sr = \frac{2\pi h}{r} sr \qquad (1)$$
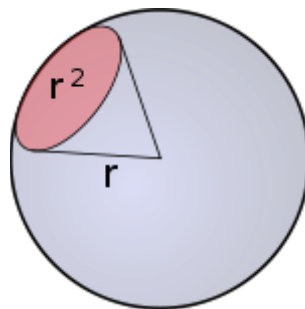
Figure 1. Steradian definition [17].

4.2 Radiant intensity

Radiant intensity is total power emitted from source per solid angle, given as watts per steradian. The total power emitted remains constant. But the power is spread over the 1 steradian cone radiation and the area increases infinitely. It is a crucial measure of a LED to know the characteristics of the light.

Two LED-s with same power characteristics might have different emitting angles. Therefore, the one with narrower beam angle will have higher radiant intensity because the power is spread out over smaller area. For LED-s the unit milliwatts per steradian (mW / sr) is usually given [16].

4.3 Irradiance

Irradiance is the power received per unit area at a certain distance. Irradiance of light is defined by the inverse square law. The further away from the source, the larger the photons are spread. The power decreases as the square of the distance as seen in the equation (2) and is measured in W/m^2 (watts per square meter), where I is radiant intensity, D is the distance and E the calculated irradiance. That means by sensing power from double the distance, the sensed power will fall four times [16]. It applies to all radiated electromagnetic energy – visible light, infrared, radio waves, x-rays and gamma rays.

$$E = \frac{I}{D^2} \tag{2}$$

4.4 Disturbance sources

For successful communication over the air, the signal needs to be distinguishable from the noise. There are multiple noise sources that increase the noise level in infrared spectrum.

The sunlight is the main disturbance source outside. As seen in Figure 2, it is the most active in the visible spectrum (400 – 700 nm) between the ultraviolet and infrared spectrums. But it still is does have considerable irradiance in the near-infrared (700 nm – 1400nm) spectrum as well.

The most irradiance to the infrared spectrum comes from the incandescent light bulbs. Meanwhile, the fluorescent lamps spectrum irradiance decreases when crossing from visible light to infrared section.
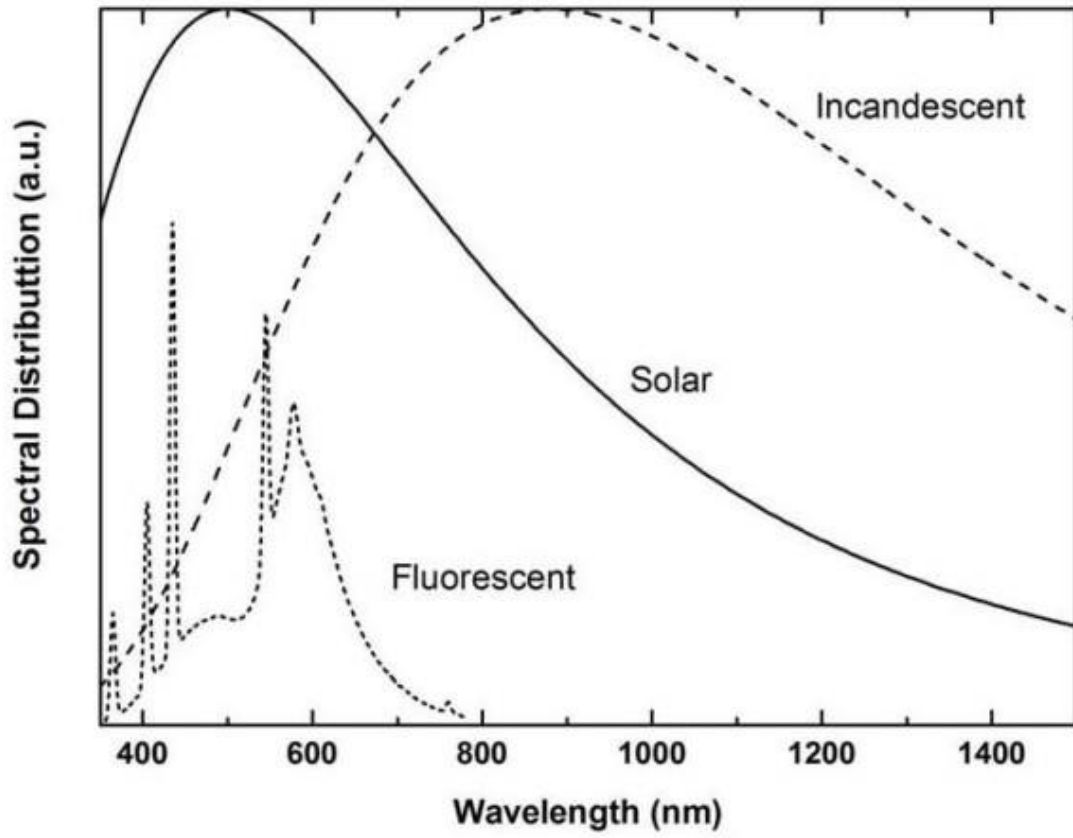
Figure 2. Incandescent, fluorescent and solar spectrum [18].

5 Design concept

The logging system is designed so that it needs a trigger signal at the lap detection point. The information must be available on the car, instead of on the track-side. The system must send out the time-critical trigger signal to CAN bus and digitally for possible future systems compatibility.

5.1 Architecture

5.1.1 Proposed concept 1

The proposed lap timing system consists of a beacon and a receiver. Beacon is a device that transmits a specific code continuously related to its location on track (lap time or split time) via infrared light. While the beacon is located track-side, the receiver is located on the car. The receiver has an infrared photodiode that receives the code, detects the lap or split time and broadcasts the information to CAN bus and digital output. The described concept is shown in Figure 3.

Figure 3. Infrared beacon-receiver based lap timing system concept (not-to-scale).

To achieve the requirements in terms of reliability and accuracy, it must be designed according to the worst-case scenario. Three extreme cases can be described:

1. The car drives past at its maximum speed (120 km/h) at 1 meter from the beacon.
2. The car drives past at the maximum distance – 5 meters, with maximum speed (120 km/h).

3. The car drives past one lap at the minimum distance 1 meters and next lap at 5 meters.

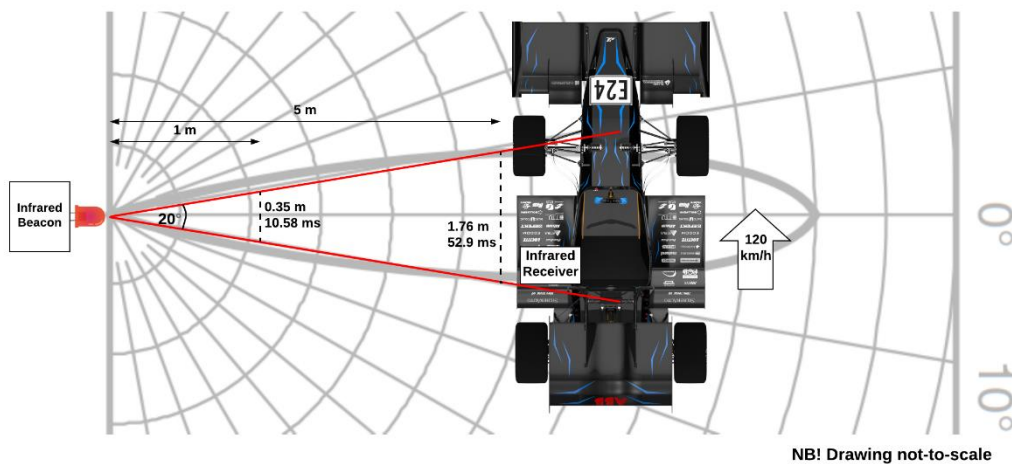The first scenario is extreme because of the beam angle of the beacon. At 1 meter distance, the distance and thus time spent at the beam is the lowest. The distance spent in the beam in that case is 0.35 m, as shown in Figure 3, which at maximum speed 120 km/h corresponds to 10.58 milliseconds of time for receiver to receive the code sent by the beacon. To receive at least one code, at least 200 Hz code transmitting frequency must be designed. To account for any unexpected events that lead to unreceived codes and to improve accuracy, even more frequency should be desired.

The second scenario is crucial because of the maximum communication distance between the beacon and receiver. It is dependent on the beacon's radiant intensity and receiver's sensitivity. Outside environment, such as sunlight or rain, also plays a big part in maximum distance. The system should be designed in a way that communication distance of 5 meters should be achievable in harsh conditions.

The third scenario creates a lap time error due to infrared beam not being straight. The first lap would be detected at 1 m 5.29 ms earlier than middle of the infrared beam and second lap is triggered at 5 m 26.45 ms earlier than centre of the beam. This already adds up to 21.16 ms of inaccuracy of lap time measurement at 120 km/h. With lower car speeds, this inaccuracy would increase significantly. Not considering the fact that the real trigger point for lap time is always before the centre of the beam.

5.1.2 Proposed concept 2

To tackle this issue, another solution is proposed, where half of the beam is blocked. That creates a straight beam from one direction, and the other direction would remain the same as seen in Figure 4.
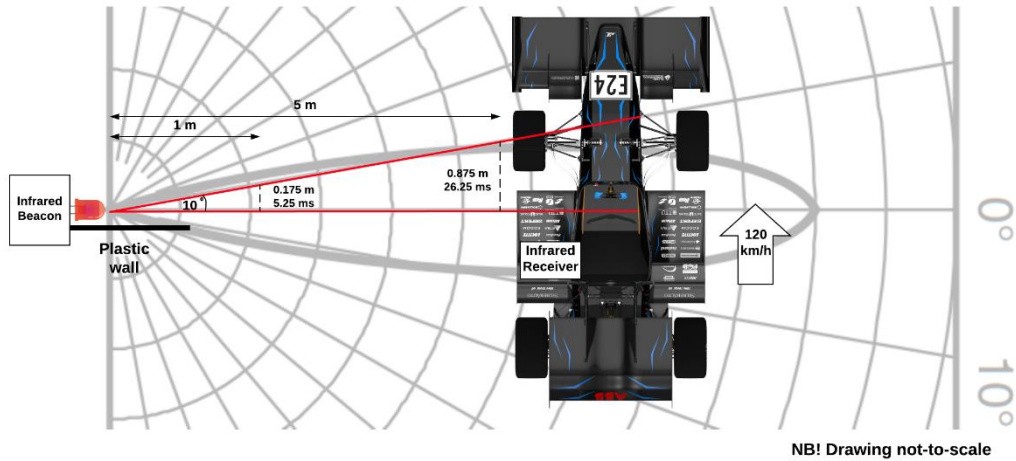
Figure 4. Infrared based lap timing system concept with half of IR beam blocked (not-to-scale).

In comparison to the previous concept, the inaccuracies of the third scenario are eliminated. But the time spent under the infrared beam is reduced by half, which is critical to assess with final beacon code transmitting frequency.

With new concept, there is 5.25 ms of time to capture the signal from the beacon when driving past beacon at 1 m distance at 120 km/h. Beacon transmit code period of at least half of the 5.25 ms is needed to ensure that code is captured at least once. Which translates to 2.625 ms period, converted to frequency of 380.95 Hz. However, to increase reliability, higher frequency is desired.

5.2 Testing

Before the design of a system, some basic tests were done on breadboard to validate the concept. At first different data formats were tested to find the most suitable coding. Then the infrared LED burst duty cycle was verified at different distances and angles.

5.2.1 Coding

There are a lot of ways to represent a bit in infrared communication. Different options of Pulse Code Modulation (PCM) are used to achieve reliable and power saving communication.

Infrared LEDs and phototransistors are fast devices and therefore, the data transmission distance is determined more by the transmit LED peak current instead of mean current. By using multiple current bursts power can be saved compared to continuous signal, while

maintaining the same working distance [19]. The burst signal and respective output of the receiver is shown in Figure 5.
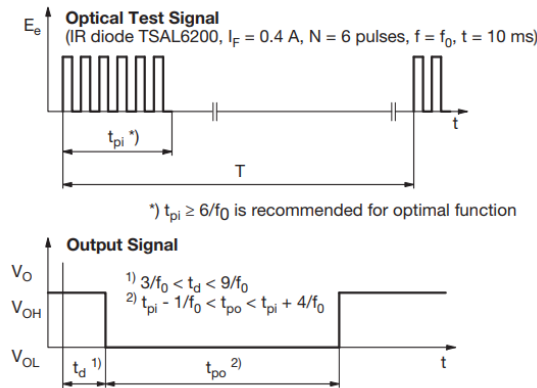
Figure 5. PCM coding and corresponding output [20].

Pulse distance coding with 2-bit codes was tested with STM32 NUCLEO-F401 development board as receiver and STM32F4DISCOVERY development board as beacon. The coding uses a constant high burst and changing delay time between 2-bits as shown in Figure 6. That way, by varying delay time 4 different codes can be used to implement the communication. The receiver is set up to detect rising edge GPIO interrupts and measures time between them. The time with acceptable tolerance is mapped to specific 2-bit code and a byte is received after 4 of the codes received.
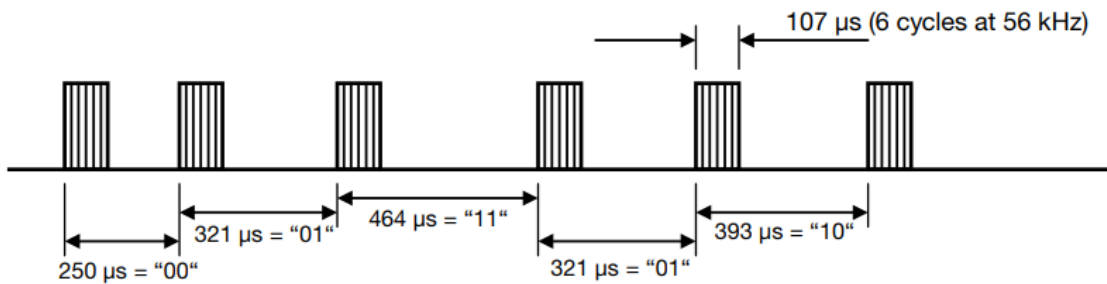
Figure 6. Pulse distance coding with 2-bit codes.

However, the received times in microseconds on the receiver fluctuated too much from the original signal to achieve reliable communication more than 100 times per second. That is lower than the minimum required frequency of 380 Hz to achieve reliable system.

Therefore, simple UART (Universal Asynchronous Receiver/Transmitter) signal over infrared, as seen in Figure 7, was tried with a specially designed infrared receiver for

25

UART communication. The crucial part of communication handling is done in hardware already in microcontroller. With that setup 580 bytes per second was achieved. With greater frequency, the receiver's built-in automatic gain control (AGC) reached its limits and therefore no signal was received continuously before transmission was interrupted [21].

As frequency of 580 Hz satisfies the final requirements and is therefore suitable communication coding for the project.

Figure 7. UART signal via infrared.

With the coding in place, the distance and angle of the LED beam was tested to validate communication in necessary points in the concept. The initial tests were done indoor to compare different receiver modules, compare different carrier duty cycles and validate the achieved distance at different angles by measuring the percentage of codes received.
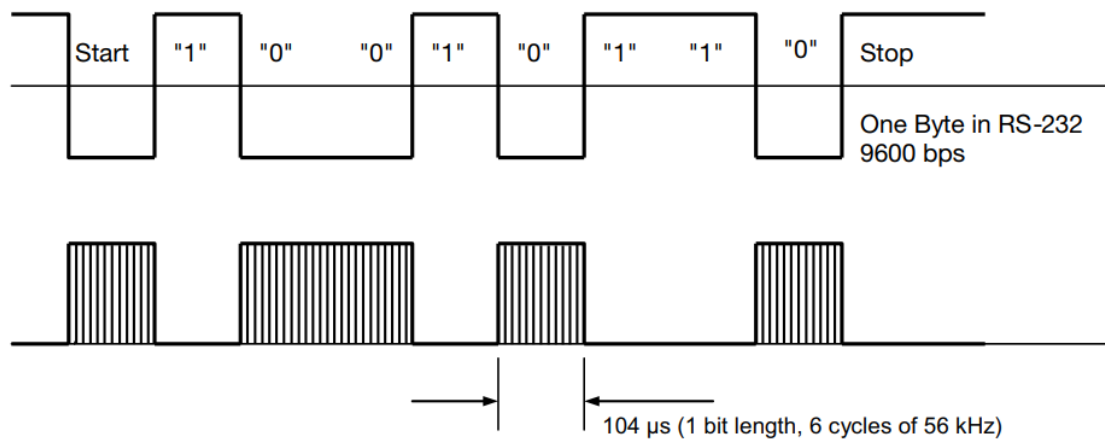
Power and therefore battery lifetime can be better saved by increasing peak IR current as opposed to increasing carrier duty cycle [22]. With 27 % duty cycle for carrier signal, the mean power was enough for all the tests to receive all the codes. But for 5 %, the distance varied for different sensors. This comes from the fact that the sensors have different band-pass filter characteristics to improve reliability in noisy environments. The TSOP4856 and TSDP34356 have the band-pass filter quality factor of 10, while TSDP34156 has 7. That means the first two filter out a narrower bandwidth and are more resistant to noisy environments. The results show the best distance achieved with the TSOP4856. The reason is that receiver TSOP4856 has lower typical minimum irradiance compared to TSDP series receivers (0.12 mW/m^2 compared to 0.15 mW/m^2) so it can detect smaller irradiance [20], [23]. The comparison of the receivers tested is shown in Table 3.

Table 3. Comparison of infrared receivers tested [20], [23], [22].

Sensor	TSOP4856	TSDP34156	TSDP34356
Carrier frequency (kHz)	56	57.6	
Quality factor	10	7	10
Minimum Irradiance (mW/ m²)	0.12	0.15	
Wavelength (nm)	950		
Minimum burst length	10	6	

The transmitter used was TSAL6200, which was powered with 5 V from the STM32 development board. With forward voltage of 1.35 V for LED, the voltage across the current limiting resistor is 3.65 V. With 50 Ohm resistor the current is calculated by simple Ohms law in equation (3).

$$I = \frac{U}{R} = \frac{3.65\,V}{50\,\Omega} = 73\,mA \tag{3}$$

To know the radiant intensity with different duty cycles the current needs to be multiplied with the duty cycle we get average current of 3.65 mA for 5 % duty cycle and 19.71 mA for 27 % duty cycle. By looking at the forward current and radiant intensity plot in the Figure 8, we can see that the respective output radiant intensity for 5 % duty cycle is 2 mW/sr and for 27 % it is 15 mW/sr.
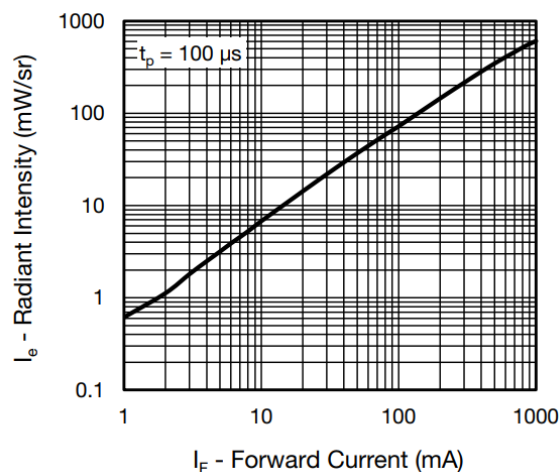
Figure 8. Forward current and radiant intensity characteristics of TSAL6200.

By combining this information to Figure 9 and using inverse square law to get irradiance at different distances, it is visible that for TSOP4856 5 % and 27 % duty cycle signals

maximum receivable distance from LED is 4 m and 11 m respectively. For TSDP series receivers, the distances for 5 % and 27 % duty cycle are 3 m and 10 m.
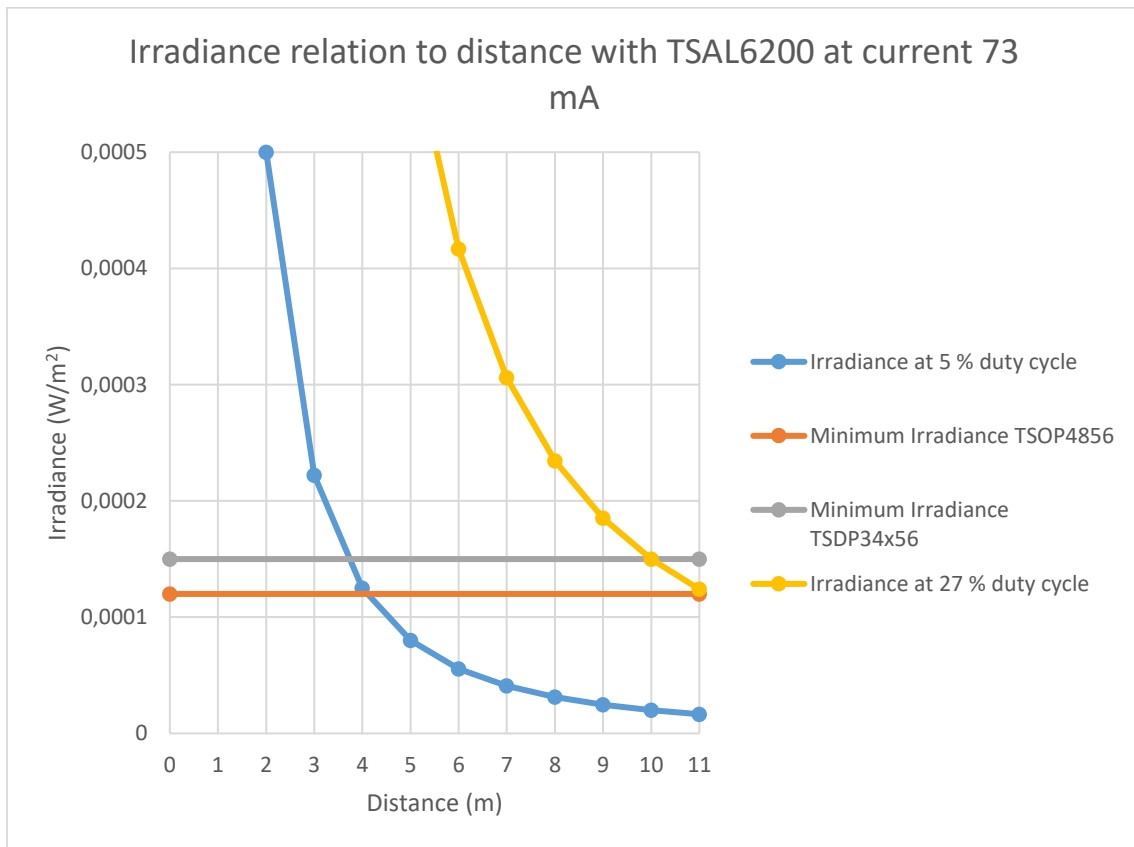
Figure 9. Radiant intensity calculation to irradiance of TSAL6200 at different distances.

The following tests are done indoor with fluorescent lights on at the room. On the floor there are markings for 1-meter increments and for 10° angle until 5 meters.

Figure 10. Led distance and angle test markings on the floor.

The calculated results and tested results are combined to Table 4. It is visible from the percentage of received codes that the received signal starts fading at 4 m for TSOP4856 and TSDP34156. For TSDP34356 the fading started at 3 m. The actual communication distance achieved during the test mostly corresponds to calculated expected values. There is even room for improvement, because room ambient light interference was not considered in this test that increases the minimum irradiance level needed by receiver.

Table 4. Percentage of received codes at different angles and distances.

	TEST 1.1		TEST 1.2		TEST 2.1		TEST 2.2		TEST 3.1		TEST 3.2	
Duty cycle (%)	5 %		27 %		5 %		27 %		5 %		27 %	
Coding	Pulse distance		Pulse distance		UART		UART		UART		UART	
Codes sent per second (Hz)	76 Hz		76 Hz		580 Hz		580 Hz		580 Hz		580 Hz	
Sensor	TSOP4856		TSOP4856		TSDP34156		TSDP34156		TSDP34356		TSDP34356	
Quality factor	10		10		7		7		10		10	
Minimum burst cycles	10		10		6		6		6		6	
Expected distance (m)	4 m		11 m		3 m		10 m		3 m		10 m	
Distance/ Angle	**10°**	**0°**	**10°**	**0°**	**10°**	**0°**	**10°**	**0°**	**10°**	**0°**	**10°**	**0°**
1 m	100 %	100 %	100 %	100 %	100 %	100 %	100 %	100 %	100 %	100 %	100 %	100 %
2 m	100 %	100 %	100 %	100 %	100 %	100 %	100 %	100 %	100 %	100 %	100 %	100 %
3 m	96 %	100 %	100 %	100 %	89 %	100 %	100 %	100 %	0 %	100 %	100 %	100 %
4 m	52 %	92 %	100 %	100 %	0 %	89 %	100 %	100 %	0 %	0 %	100 %	100 %
5 m	0 %	60 %	100 %	100 %	0 %	0 %	100 %	100 %	0 %	0 %	100 %	100 %

With reliable communication protocol and theoretical calculations verified, more tests with environment closer to the device real application were done. The main concerns in real application are detection on a moving object and sunlight interference.

The sunlight decreases receiver's gain and as a result increases minimum irradiance level as seen in Figure 11. For daylight, the ambient light in the datasheet is defined as 10 W/m^2, which results in infrared receiver minimum irradiance of ~0.12 mW/m^2 [20].
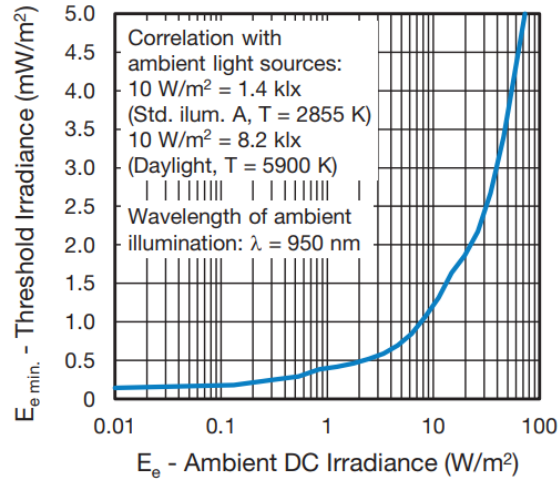
Figure 11. Ambient light relation to TSDP receiver minimum irradiance level [20].

As seen in the Figure 12, with the same current draw as in Figure 9, the 50 % duty cycle carrier signal can achieve only 4 m communication distance as its irradiance is not above the minimum irradiance of TSDP34x56 at sunlight at greater distances. Therefore, to improve maximum communication distance in final design, an infrared LED with narrower beam and thus higher radiant intensity.

Figure 12. Different duty cycles irradiance of TSAL6200 at distances compared to minimum irradiance of TSDP34x56 at sunlight.

5.3 Theoretical accuracy

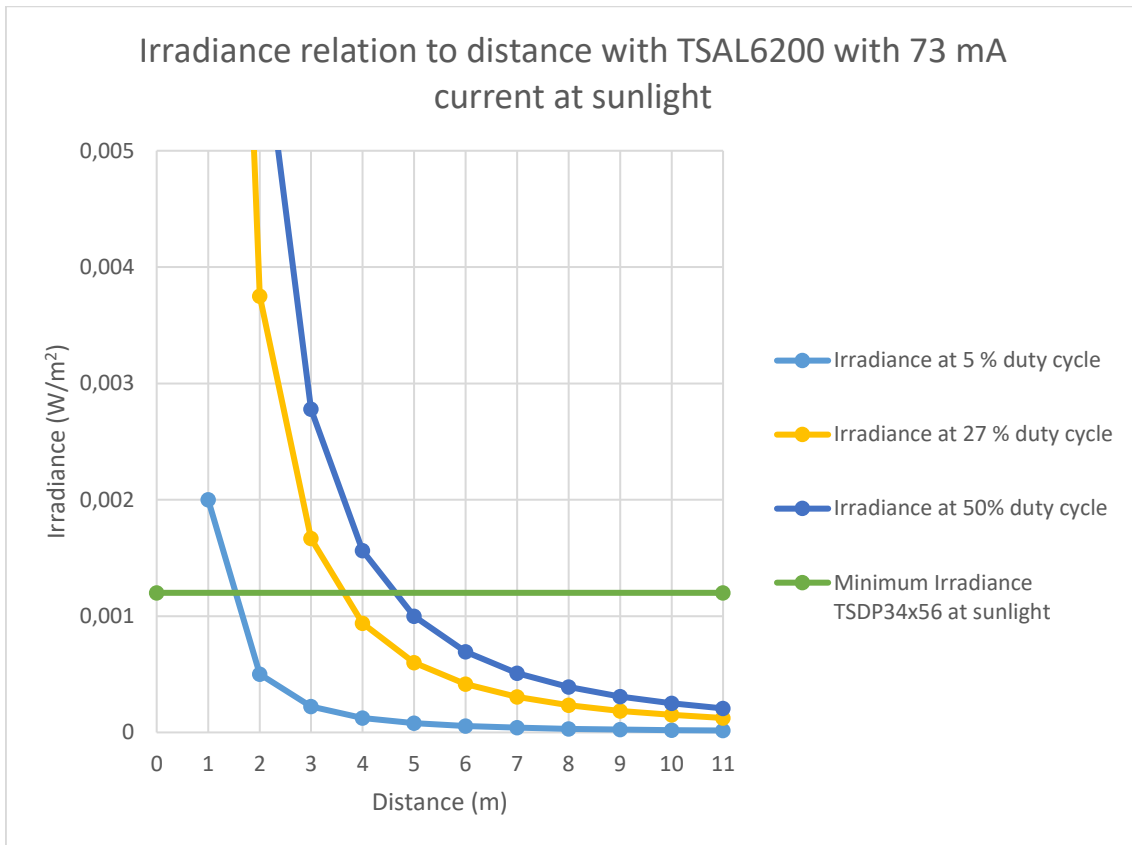To calculate the theoretical accuracy, worst case of each error source must be added up. The concept shown in Figure 4 and the beacon 580 Hz code transmit frequency are used as the basis. Constant latency sources, such as CAN message transmission, speed of light, UART message transmission are disregarded as these do not introduce noticeable variation in time thus, do not impact lap timing calculation significantly.

5.3.1 Lap detection time

Depending on the time the receiver will appear on the infrared beam, different error scenarios are possible. The worst error would happen if the receiver appears on the beam just after the code start bit is transmitted. Then the start of the next code must be waited. That makes the error time of the 580 Hz period of 1.724 ms.

5.3.2 CAN bus waiting time

After detection of the infrared coded signal, immediately CAN message is sent out. But as CAN bus is a half-duplex communication, there might be messages currently being

transmitted to the bus. The transmission must be waited until the bus is free and CAN message with the lowest ID is transmitted first as it wins the arbitration if any other node tries to transmit at the same time. This process is shown in Figure 13. The use of lowest CAN ID will be desired on the final system, depending on the nodes present on the same CAN bus.
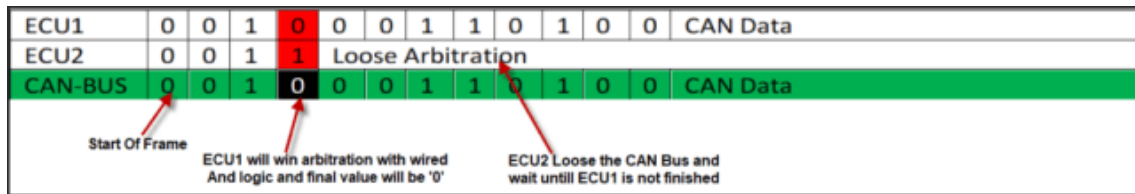

Figure 13. Arbitration for CAN ID-s [24].

The error detection mechanism of bit stuffing might add length to the CAN message. If 5 consecutive same bits are present on the data stream, the sender inserts a stuff bit of opposite polarity, which is removed by the receivers [25]. Assuming a standard message length, with 8 data bytes and maximum number of stuff bits possible, 134 bits are transmitted. With 1 Mbit/s CAN bus speed used, that accounts to 134 us of possible delay.

5.3.3 Logging time

The lap time trigger is needed for the logging system to receive and when analysed in computer program, it is recognized automatically with lap and split times calculated. The maximum logging frequency of the logger used is 1000 Hz, which contributes to 1 ms of time error.

5.3.4 Overall theoretical lap time error

Overall theoretical error is the sum of all the sub-errors, because all the inaccuracies can only add time to lap time detection in the logging system, not decrease. That makes the worst case of consecutive laps with no error and maximum error or vice versa. The distribution of errors can be seen in Figure 14, with total of 2.858 ms theoretical error and 7.142 ms of margin to target 10 ms accuracy.
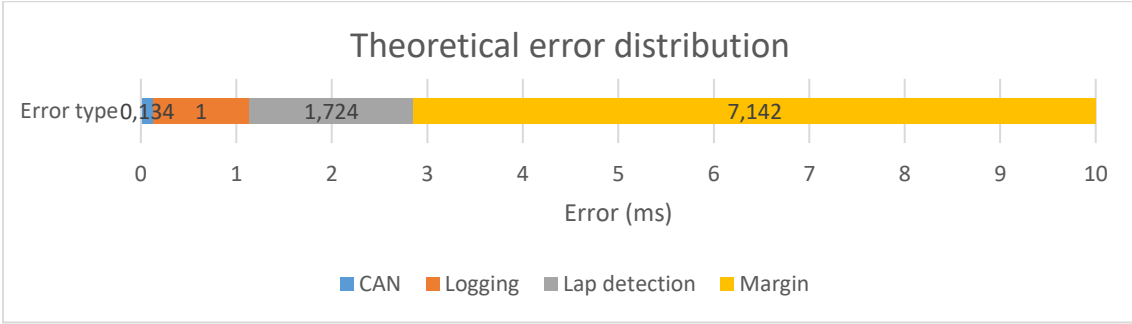
Figure 14. Theoretical error distribution.

6 Hardware

Altium Designer is used for design of electronic circuits and PCB layout. Hierarchical design of circuits is used instead of a flat design. The sheets are organized in parent-child, where child sheets define the circuits, inputs and outputs of the sheet. After that, the inputs and outputs can be connected at parent sheet. That enables design reuse and creates a good overview of the project on the parent sheet [26]. The example of flat and hierarchical design is shown in Figure 15.
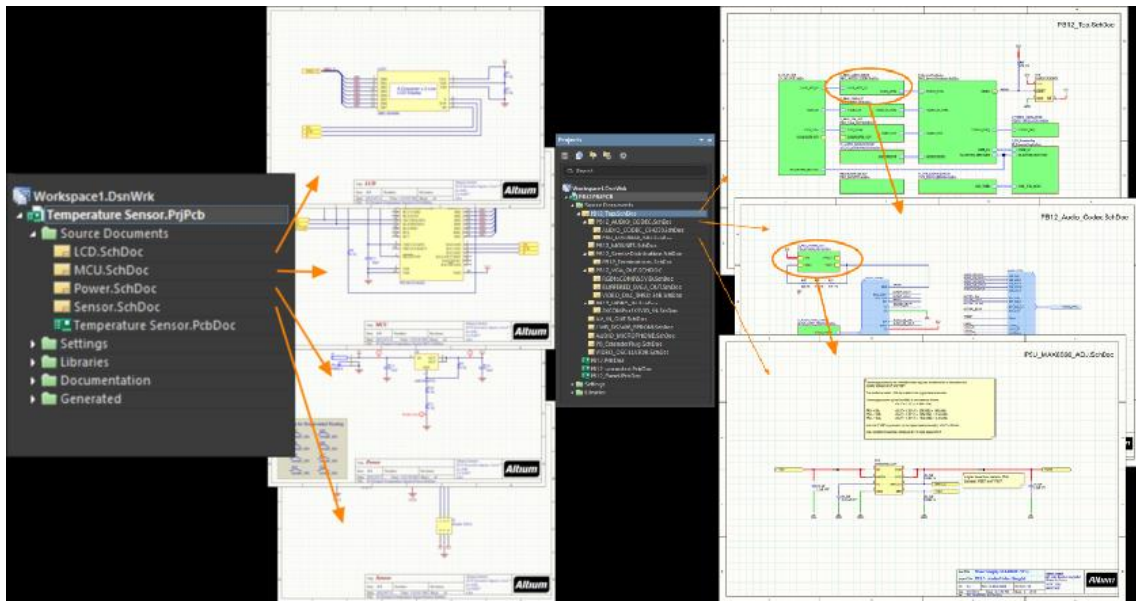
Figure 15. Flat(left) and hierarchical(right) design of electronic circuit.

6.1 Concept

The beacon design has to implement a code selection (split or lap time identification) and transmitting the code as a simple UART series bytes. The circuit is powered from battery, therefore it should be possible to know the battery level in a quick way while testing on the track and quickly adjust the maximum range (carrier frequency duty cycle) or decide if battery should be replaced.

The receiver must capture the lap/split beacon infrared signal and transmit the information to CAN bus and digital output. Since it is powered from cars 24 V system, power-saving is not a priority. The beacon-receiver concept, including the interactions with the outside system is shown in Figure 16.

Figure 16. Beacon and receiver hardware concept.
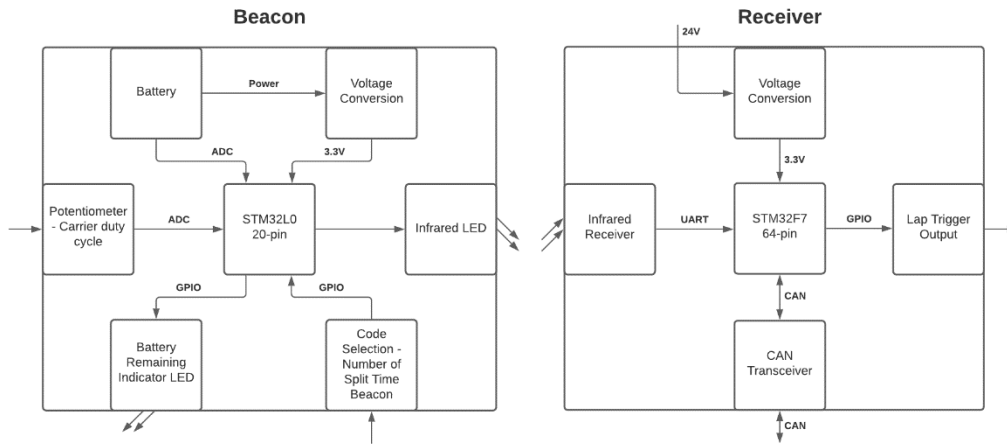
6.2 Beacon

6.2.1 Infrared LED

The main part of the beacon is the infrared LED. In the final design TSAL6100 LED is used instead of TSAL6200, having narrower beam angle (10° instead of 17°). The communication is calculated to work at 27 % carrier duty cycle but depending on the conditions it can be adjusted to more range quickly. Compared to the testing circuit, 3.3V voltage level is used on the final design. As the LED forward voltage of 1.35 V remained the same, voltage drop on the resistor is 1.95 V. The current draw of the 25 Ω current limiting resistor is calculated by Ohm's law by dividing voltage drop on resistor to resistance, which calculates to 78 mA. Resulting distances using TSAL6100 at 78 mA are shown in Figure 18.

The resistors power rating must be at least 152.1 mW, thus resistor with 250 mW power rating is chosen. The schematic is shown in Figure 17. The calculated maximum communication distance at different duty cycles for TSAL6100 infrared LED is shown in Figure 18.
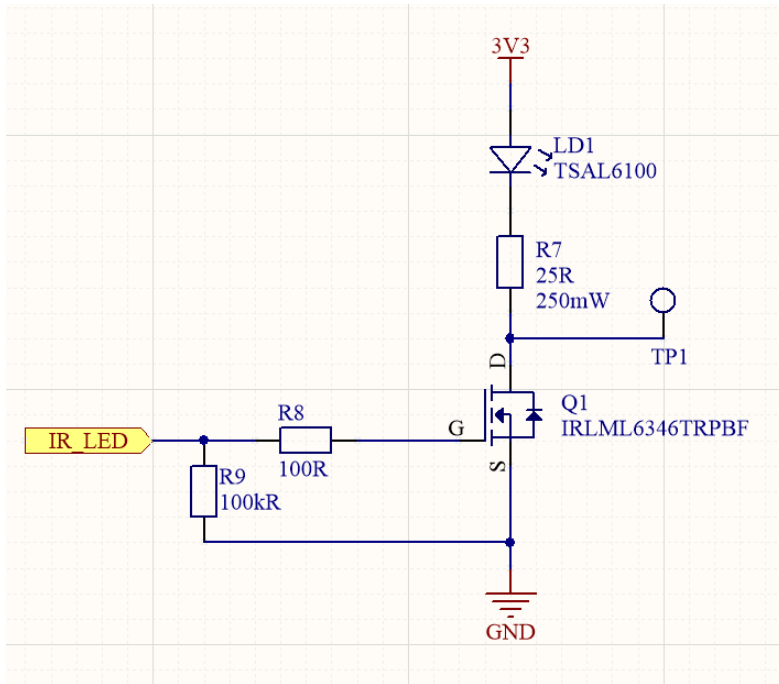
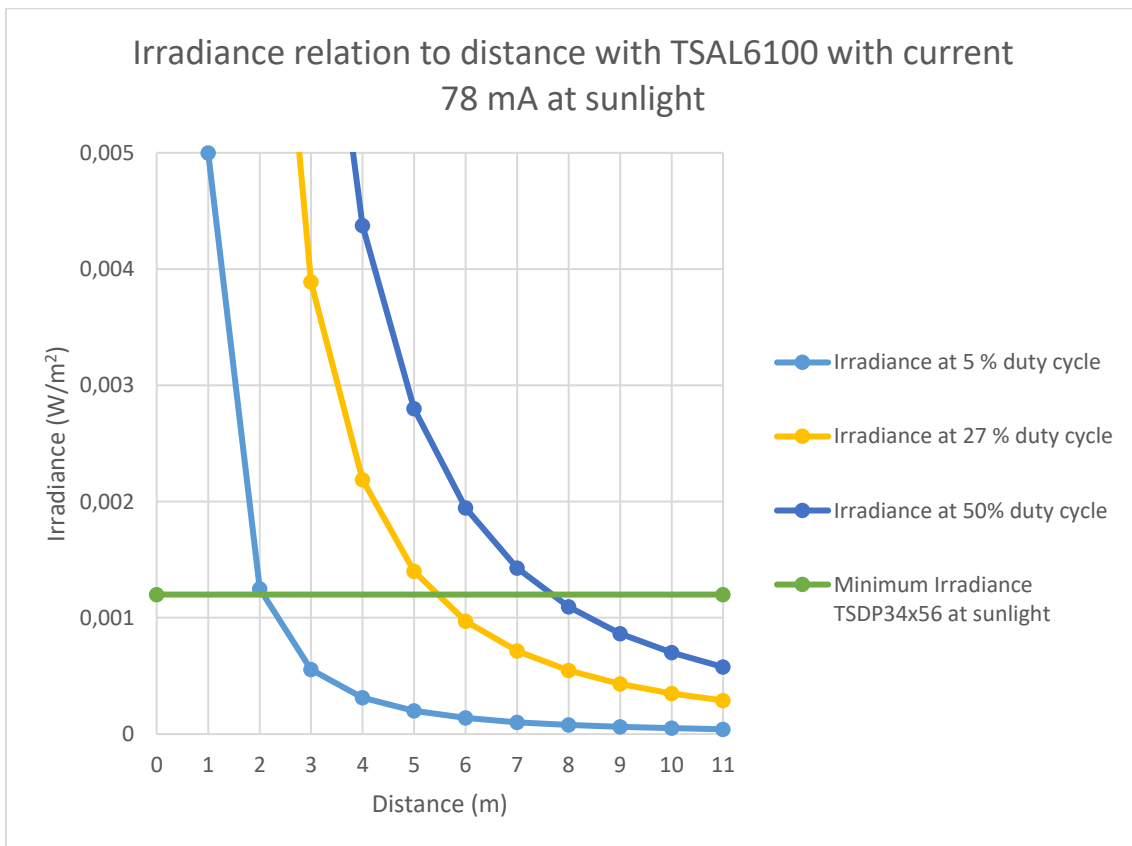Figure 17. Infrared LED switching schematic.

Figure 18. Different duty cycles irradiance of TSAL6100 at distances compared to minimum irradiance of TSDP34x56 at sunlight.

The switching is done by n-MOSFET IRLML6346TRPBF from International Rectifier. It has drain-source breakdown voltage of 30 V, which is significantly more than 3.3 V. The gate is pulsed by microcontroller with 3.3 V, which is greater than the threshold voltage 800 mV. That makes the drain-source on resistance $R_{DS(ON)}$ to ~52 mΩ, which is again, not significant compared to 25 Ω series resistance already in the circuit.

To calculate the rise time of the transistors gate, the gate charge is taken as close as possible from the Figure 19. The closest charge it is possible to get from the plot is for 6 V drain-source voltage, which is ~3 nC. The gate internal resistance is rated at 3.9 Ω and a series resistance R of 100 Ω is in series with the gate to reduce inrush current which adds up to 103.9 Ω gate resistance. The gate capacitance can be calculated at 3.3 V with the equation (4).

$$C_G = \frac{Q}{V} = \frac{3\ nC}{3.3\ V} = 909\ pF \tag{4}$$

Time to reach the gate-source threshold is given in equation (5) [27].

$$t = (R \times C_G) \times \ln\left(\frac{V_G}{V_G - V_{TH}}\right) = (103.9\ \Omega \times 909\ pF) \times \ln\left(\frac{3.3\ V}{3.3\ V - 0.8\ V}\right) = 26.2\ ns \tag{5}$$

The carrier signal length is ~18 us and when duty cycle is adjusted to 5 %, 900 ns pulse is the most critical rise time in the circuit. Rise time of the MOSFET accounts for 2.9 % of the shortest pulse, which is acceptable. Additionally, a 100 kΩ pull-down resistor is at the gate to keep the signal low when it is not driven.
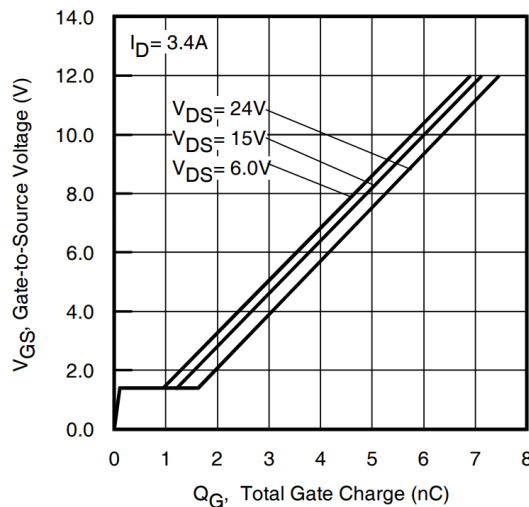
Figure 19. IRLML6346TRPBF gate charge plot [28].

6.2.2 Microcontroller STM32L0

In microcontroller selection, previous experience with STM32 series was considered. The microcontroller should be low-power and include 2 ADC channels, timer capable of outputting the carrier frequency and 9 GPIO pins used for code input and LED interface for user. STM32 has a wide range of products with different applications, including low-power series, which is a good fit for this application. Different STM32 series MCU-s are shown in Figure 20.
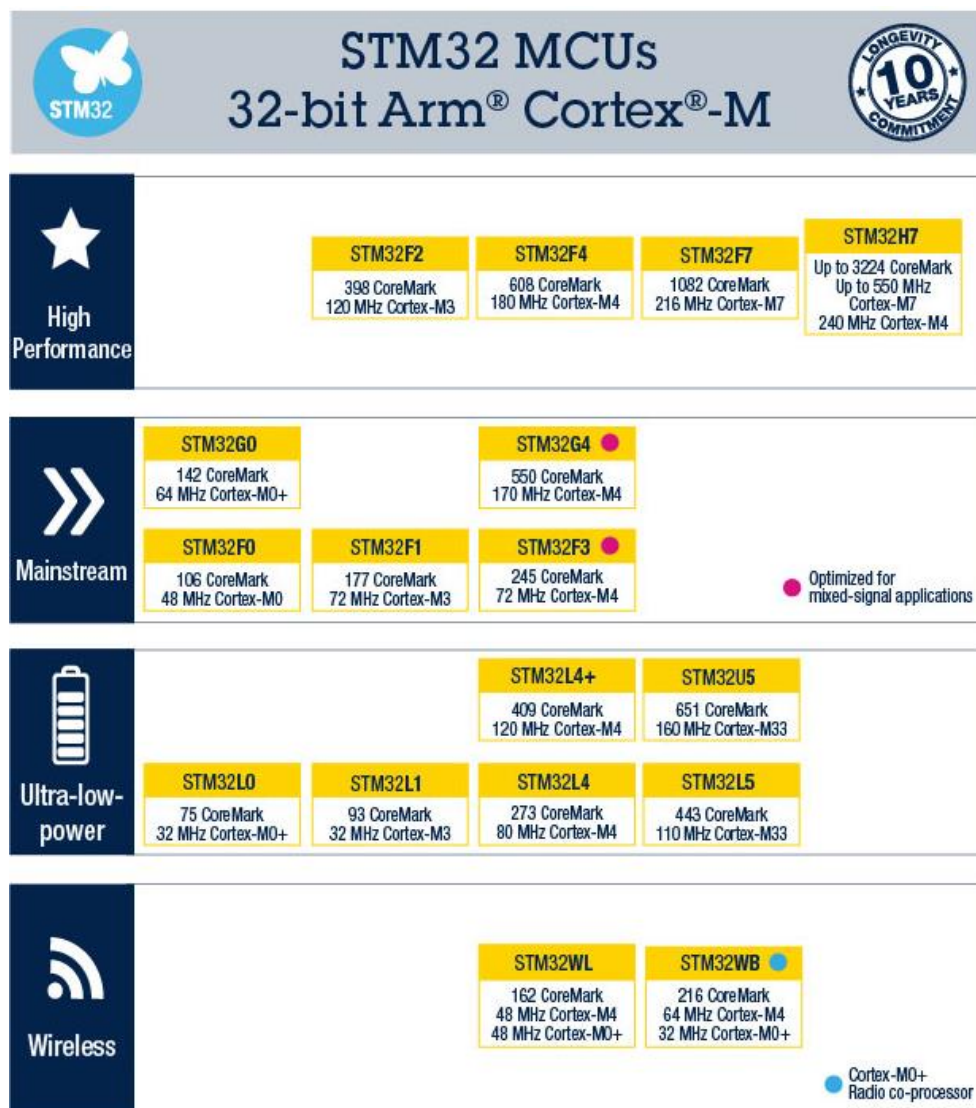
Figure 20. STM32 series microcontrollers [29].

The most low-power and low-performance MCU was chosen due to soft real-time system application. STM32L031F6 with 20-pin TSSOP package was selected due to availability

and ease of soldering manually. As shown in Figure 21 and Figure 22, after using 2 additional pins for programming and debugging purposes, only one pin was left unused.
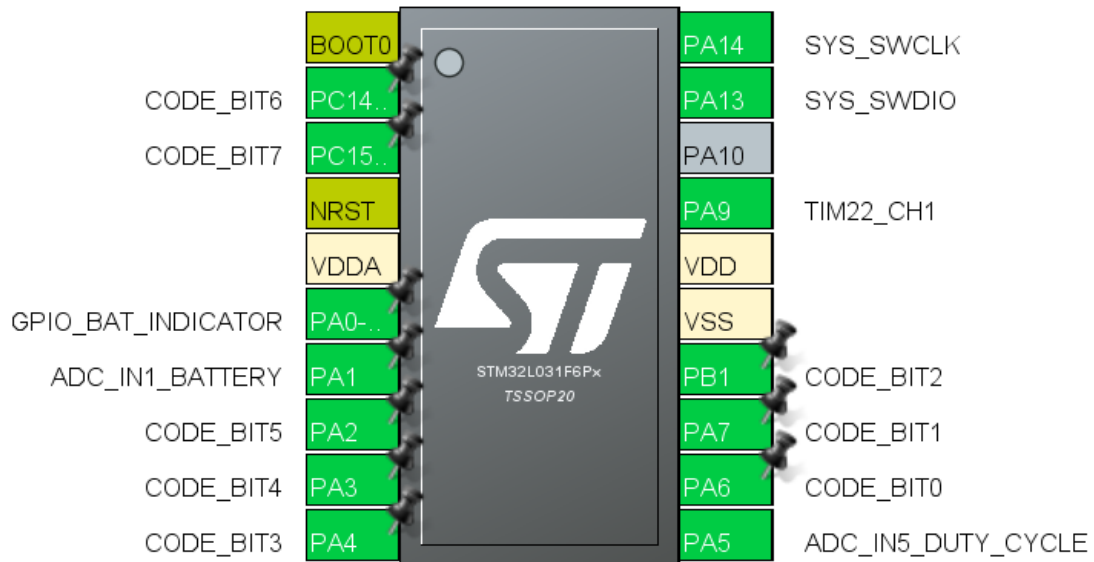
Figure 21. STM32L031F6 pinout in STM32CubeMX.
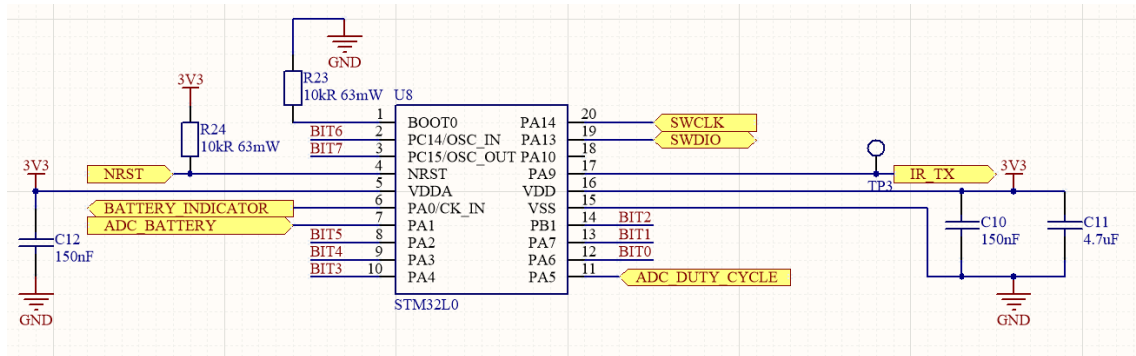
Figure 22. Microcontroller circuit in Altium Designer.

6.2.3 Additional circuits

Additionally, if it becomes necessary at different sunlight conditions to increase the infrared LED light intensity, it can be controlled via the potentiometer. It is read by the microcontroller ADC which in turn changes infrared LED duty cycle accordingly, thus increasing/decreasing the maximum communication distance.

Also, a LED to indicate the battery state of charge to user is included and microcontroller programming connector to enable STM32L0 debugging over SWD (Serial Wire Debug) interface. These are shown in Figure 23.
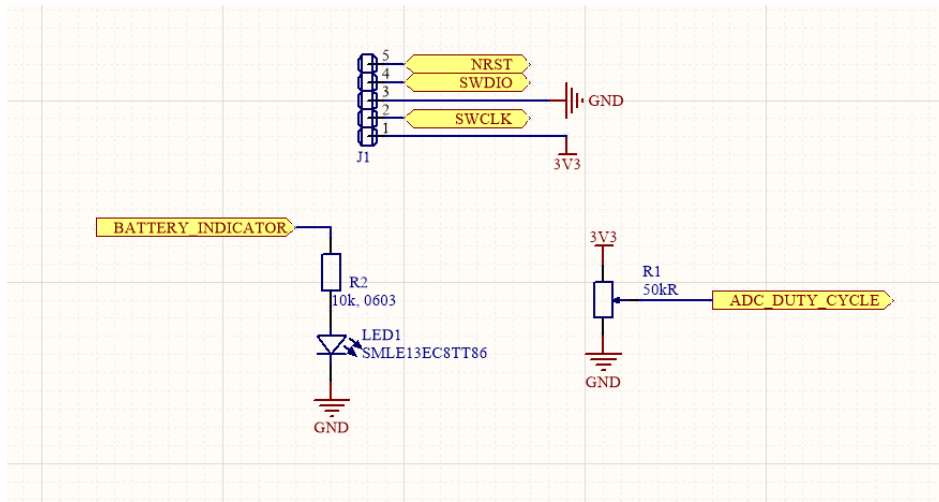
Figure 23. Additional circuits/components.

To distinguish lap and split time beacons, a code can be selected by DIP (dual in-line package) switch. The bit signals are pulled up by 100 kΩ resistors shown in Figure 24 and read by the STM32L0.
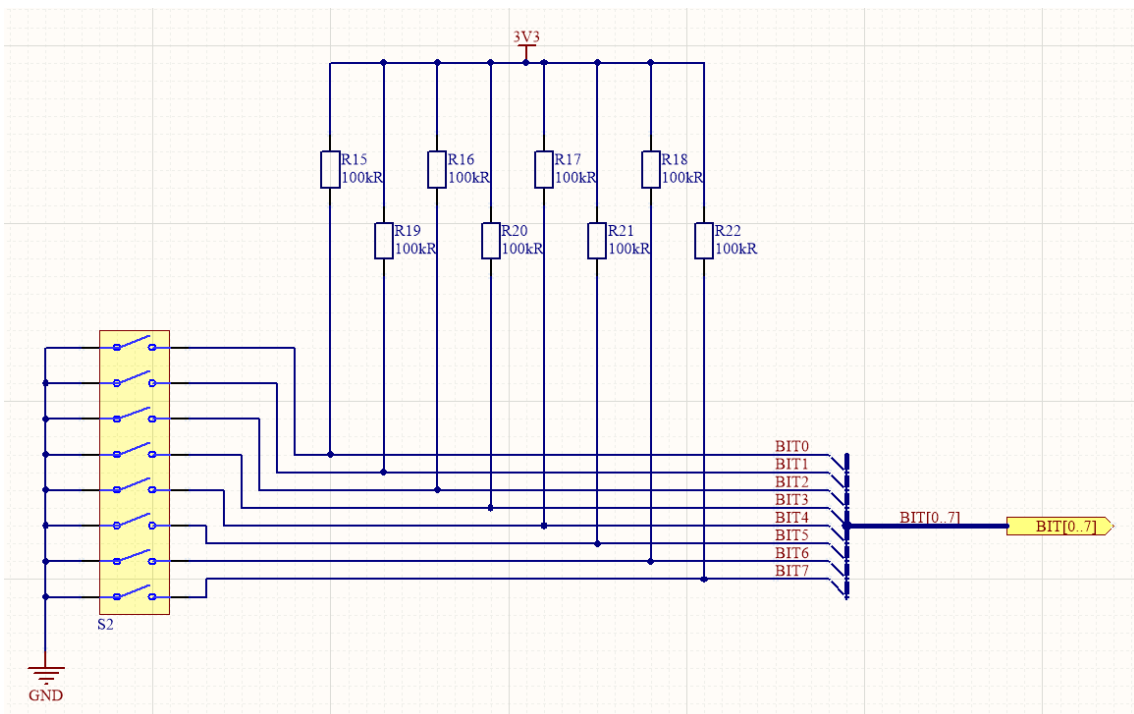
Figure 24. Code selection circuit.

6.2.4 Power and battery

Firstly, to choose battery, estimated power usage needs to be calculated to achieve the targeted 24-hours continuous working time. For that, estimated current consumption was calculated for main components.

The microcontroller's current consumption was estimated with STM32CubeMX Power Consumption Calculator. It takes 6 carrier cycles at 57.6 kHz frequency to represent one bit via infrared LED. Adding the UART start and stop bit, code consists of 10 bits. And the time it takes to transmit is calculated in equation (6).

$$t = 6 \; carrier \; cycles \; \times \frac{1}{57600 \; Hz} \times 10 \; bits \; = 1.042 \; ms \qquad (6)$$

The STM32L0 is using minimal peripherals required for operation and is using running and sleep states to save energy. It is assumed that STM32L0 at running state is at maximum 16 MHz internal clock and is using GPIOA, GPIOB, GPIOC, TIM22, ADC and runs for 1.042 ms. The sleep state should last between end of code transmission and start of transmission of next code. Therefore, sleep state duration equals to code transmission period subtracted by time to send one byte as calculated in (7). The sleep state uses minimal clock of 4 MHz and runs for 0.682 ms.

$$t = \frac{1}{580 \; Hz} - \; 1.042 \; ms = 0.682 \; ms \qquad (7)$$

This results in 2.51 mA current consumption at run state and 0.181 mA at sleep state. Considering the timings of states, average current resulted in 1.59 mA as shown in Figure 25. This could be later optimized in software by de-initializing some peripherals after it has been used at start-up. For example, ADC can be de-initialized after battery voltage and desired duty cycle are measured.
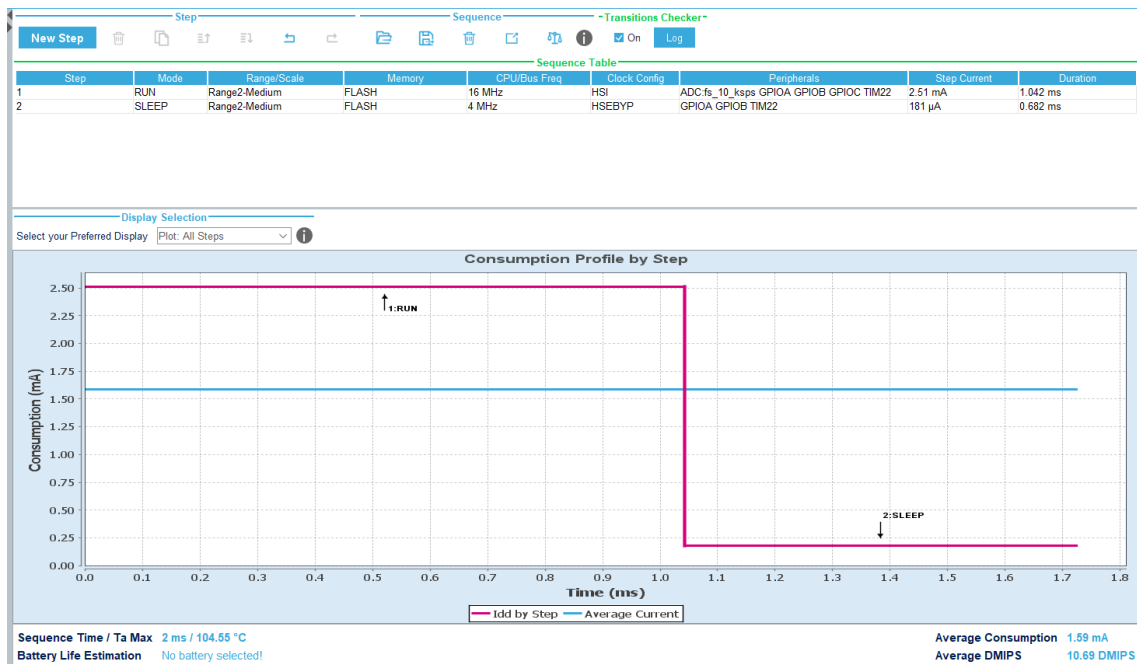
Figure 25. Run and sleep state current consumption estimation using STM32CubeMX.

Infrared LED is the biggest power consumer in the PCB. Assuming all the bits transmitted, including start and stop bit are high, the worst case current consumption of LED can be calculated as in equation (8). The duration of one UART byte is multiplied by number of codes transmitted in a second and multiplied with the worst case duty cycle of 50%.

$$t = 1.042 \, ms \, \times 580 \, Hz \, \times 0.5 = 302.18 \, ms \tag{8}$$

The main current consumers of the circuit are defined in Table 5. The current consumption is converted to power draw to take into account the battery voltage measurement resistor divider, which works at battery voltage, not 3.3 V supply. Additional circuits, such as 50 kΩ potentiometer and various pull-up resistors are considered in the table as well. Power draw is added up to determine the battery capacity needed to achieve at least 24-hour working hours.

Table 5. Current consumption of beacon circuits.

Name	Voltage (V)	Current (mA)	Power (mW)
IR LED	3.3	23.56	77.76
Microcontroller	3.3	1.59	5.25
Battery voltage	9	0.07	0.62
Pull-up resistors	3.3	0.26	0.87
3V3 LED	3.3	0.03	0.10
Potentiometer	3.3	0.07	0.22
Total			**84.81**

To calculate runtime with 84.81 mW for different batteries, equation (9) is used.

$$t = \frac{E}{P} \tag{9}$$

Using typical battery capacities, battery runtime is calculated and shown in Table 6. [30] Both, AA and 9V battery ensure the necessary runtime required. 9V type is chosen because of simple and efficient buck (step-down) converter can be used then to convert 9...6V to 3.3V while also providing the most runtime.

Table 6. Battery runtime calculation [30].

Battery type	Capacity (Wh)	Runtime (h)
AAA	1.725	20
AA	4.275	50
9V	5.13	60

An easy-to-use synchronous buck converter LMR50410 is chosen because of relatively good efficiency and simple physical SOT-23-6 package [31]. At 8V input voltage, ~8 mA is drawn continuously, which looking at Figure 26 makes the efficiency close to ~90 %. Considering the efficiency, more precise runtime estimation is 60 h x 0.9 = 54 h.
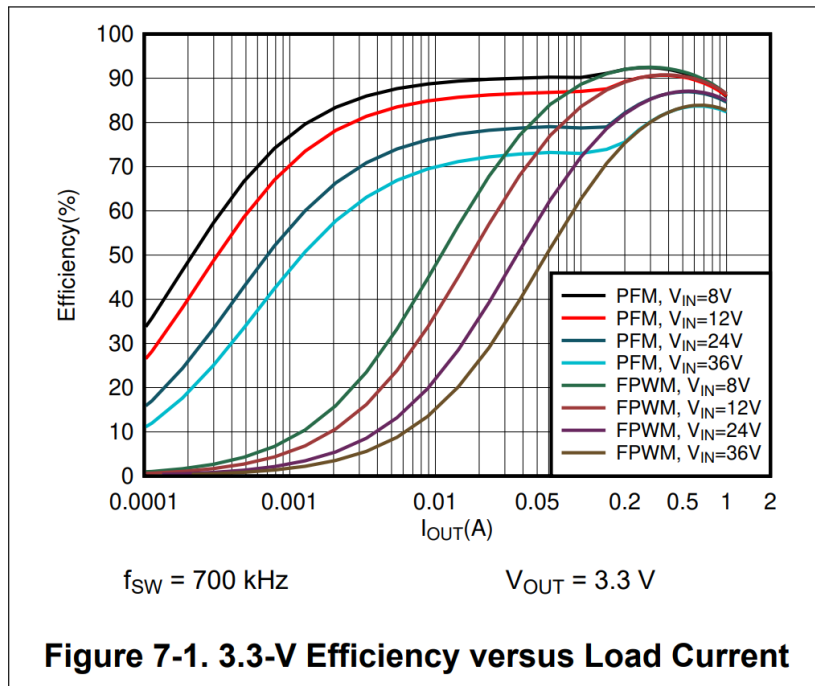
Figure 26. LMR50410 efficiency with 3.3V output.

Power conversion circuit is done according to suggestions of the buck converter datasheet. It includes a resistor divider for measuring battery voltage and an LED to indicate the 3.3 V supply voltage presence. The resistor divider is relatively high resistance to save battery energy, as it is continuously drawing current.
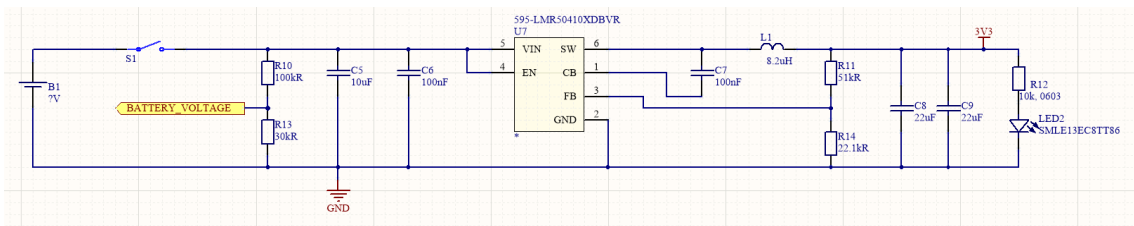
Figure 27. Battery and power conversion schematics.

6.3 Receiver

6.3.1 Infrared receiver

Previously tested TSDP34156 is used in the final design because of its compliant filter that enables to achieve required code transmitting frequency. As shown in Figure 28, the incoming infrared signal is firstly received by the photodiode and the AC part of the signal is passed to transimpedance amplifier. There, the signal current is converted to voltage to

45

the input to controlled gain amplifier where most of the gain in the system is generated, controlled by AGC (automatic gain control) feedback [22].

Next, signal is passed through band-pass filter to get good performance at noisy environments. In case of TSDP34156, it is tuned to center frequency 57.6 kHz which is used as a carrier signal frequency. AGC adjusts the system sensitivity according to the existing noise or disturbance level by adjusting gain of the amplifier, thus ensuring reliable communication at various conditions. In dark ambient, the gain is set to most sensitive value at which there are no random output pulses [22].

From there, signal is passed to ATC (automatic threshold control), where signal is compared to threshold level currently set. When a signal is received, threshold is adjusted to higher value, preventing any random pulses being passed and keeping threshold level above noise floor. The comparator threshold goes back to initial value after approximately for 10 ms any signal has not been received [22].

If the signal is above the comparator threshold, the integrator is triggered. Multiple consecutive triggers are required for finally triggering the device output. The integrator prevents passing spikes to the output. The combination of integrator and Schmitt trigger is optimised so that the input optical burst length is close to the output pulse width. The digital output of the device is an open collector transistor with an internal pull-up resistor [22].

BLOCK DIAGRAM
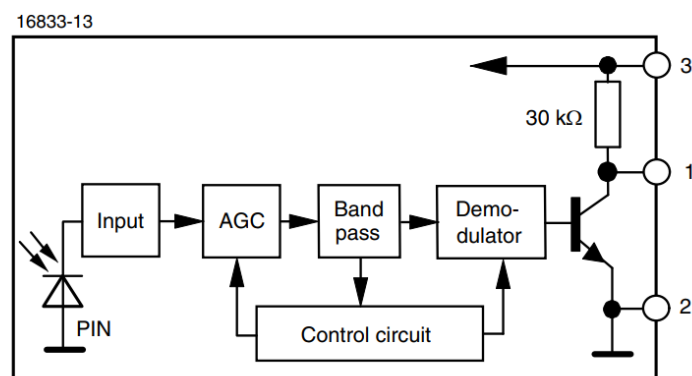
Figure 28. Block diagram of TSDP34156 [20].

With the necessary filtering done inside the IR receiver itself, the circuit to get the UART signal to microcontroller is as simple as shown in Figure 29. A recommended bulk capacitor is added to ensure reliable voltage supply for the receiver.

46

Figure 29. TSDP34156 IR receiver circuit.

6.3.2 Microcontroller

The microcontroller must receive the infrared signal via UART, transmit CAN signals, trigger digital lap time trigger. Also ease of solderability and previous experience with programming was considered. STM32F7 series with the least pins available was chosen because of its good performance for the price. Also, power-saving is not a priority because the board is supplied by the formula student car DCDC (DC-to-DC converter) that takes its energy from high voltage battery.

The necessary bulk and decoupling capacitors are added according to STM32F7 datasheet [32]. As seen in Figure 30, most of the pins remain unused.

Figure 30. STM32F730R8T6 surrounding circuit.

6.3.3 Isolated CAN bus

Previous experience with electric formula student cars has introduced a lot of CAN bus problems due to high EMI (electromagnetic interference) from the electric motor inverters and high voltage cabling. For that reason, isolated CAN bus topology is used wherever possible, mitigating the disturbance from the traction system.

Selected signal and power isolated CAN transceiver ADM3053 features iCoupler and isoPower technology to isolate the CAN bus and application side. The design is compactly fitted to one chip, requiring only external bulk and decoupling capacitors and ferrite beads for high frequency noise suppression [33].

The needed external components are seen in Figure 32. Additionally, an option to connect a split termination is added which can be switched by DIP switch. Split termination improves filtering of high frequency common-mode noise with a coupling capacitor at the center-tap of two 60 Ω resistors. Example of the split termination filtering effect can be seen in Figure 31 [34].
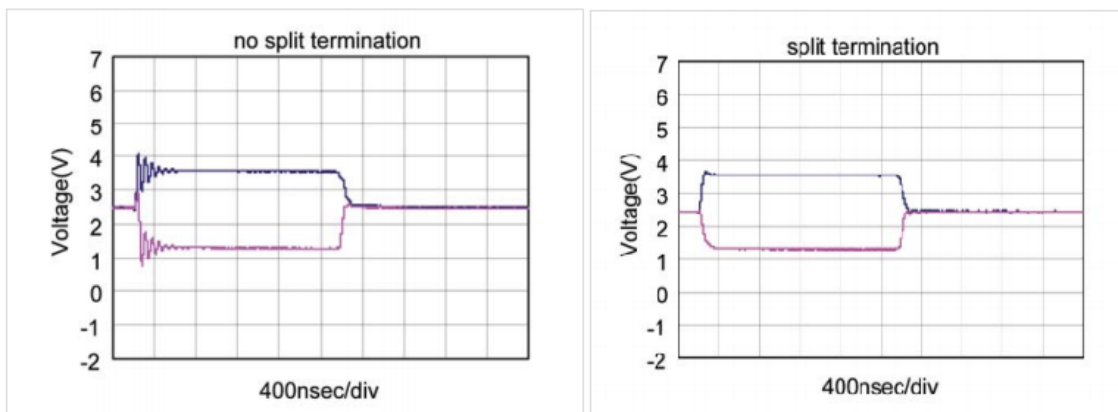

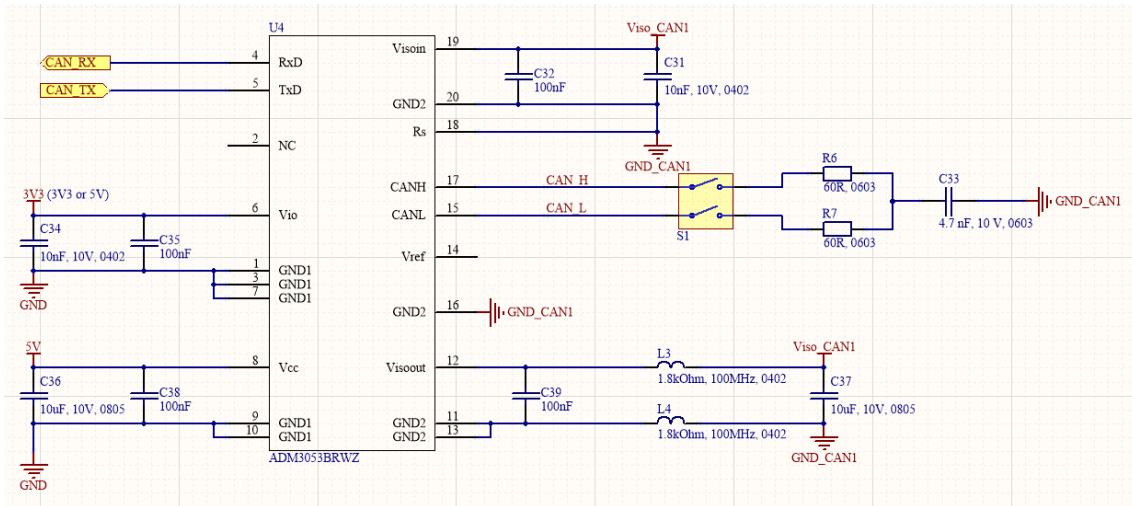Figure 31. Split termination effect on CAN bus common-mode noise [34].

Figure 32. Isolated CAN bus transceiver circuit.

6.4 Result

Both of the PCB-s have an enclosure designed by other FS Team Tallinn members to protect against water or any other possible environment impact. The beacon will be fastened to a tripod for stable platform throughout a test day and placed next to track facing track-side. The receiver will be fastened outside of formula student car chassis.

The receiver and beacon design with and without an enclosure can be seen in Figure 33. The infrared beam blocking wall is seen in (b1). It is built in a modular way, such that the wall is detachable and can be mounted on the other side of the infrared LED quickly, depending on the track position.
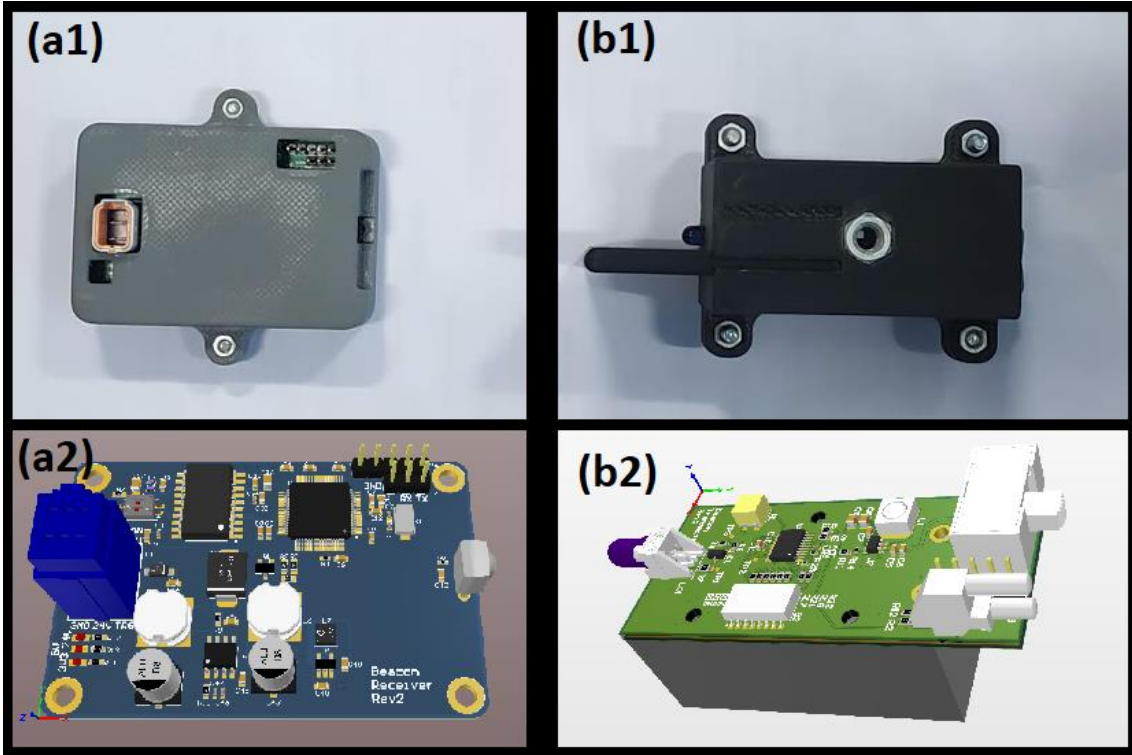
Figure 33. The receiver PCB 3D (a2) and with enclosure (a1). The beacon PCB 3D (b2) and with enclosure (b1).

7 Software

To ease software development on STM32 devices, STMicroelectronics have developed Hardware Abstraction Libraries (HAL), thus reducing development effort, cost and time. HAL is a high-level functional abstraction, that enables portability across all STM32 devices and is available for all peripherals. User code is on top of the HAL and possible STM32 middleware, if used. HAL is based on Low-Layer (LL) API, that is fast and light-weight hardware layer. High portability and abstraction however create more overhead code, thus taking more time executing the code. The architecture provided by STMicroelectronics can be seen in Figure 34 [35].
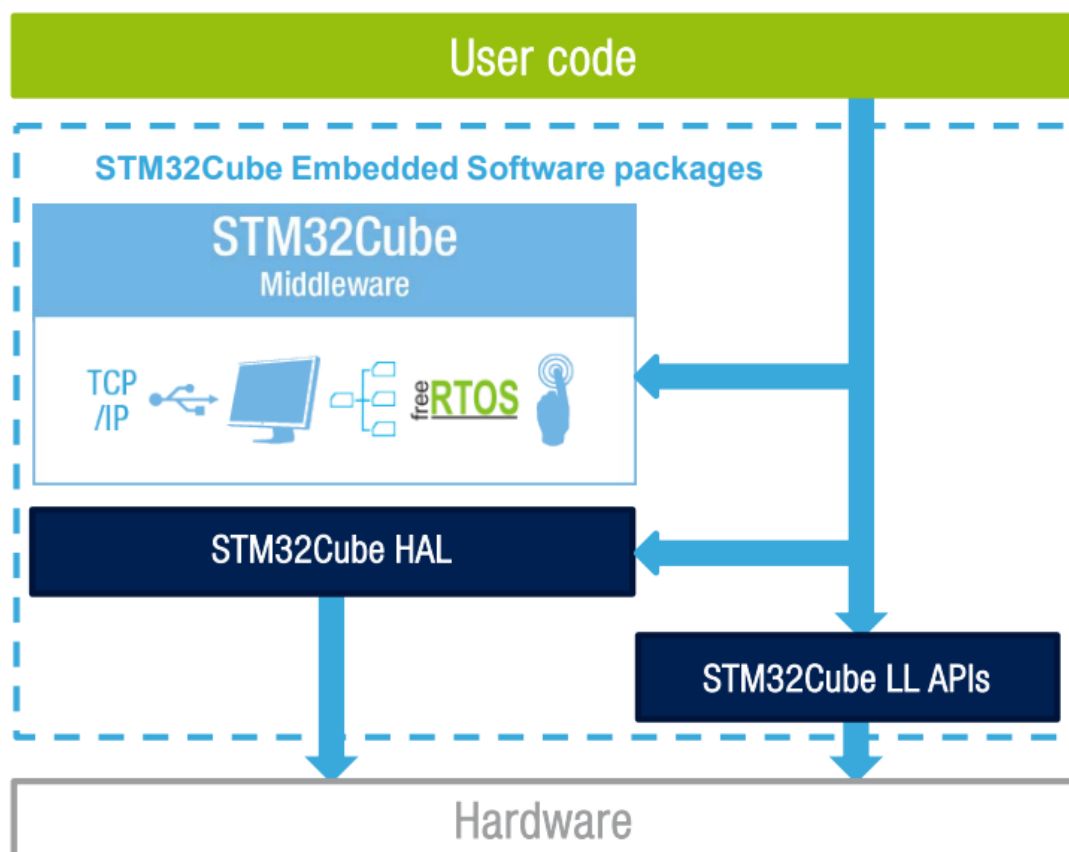
Figure 34. STMicroelectronics architecture [36].

7.1 Beacon

The input clock for the timer 22 on the STM32L03 is 32 MHz coming from APB2 (Advanced Peripheral Bus). The needed timer frequency is the carrier frequency of the infrared receiver, which is 57600 Hz. As seen in the Figure 35, input frequency is divided by the PSC (prescaler register) and by that interval, a CNT (counter register) is counted until ARR (auto-reload register) value is reached. The timer frequency is calculated in equation (10). The values are chosen to get the best match, which ended up being 371 Hz off the desired value.

$$f = \frac{TIM\_CLK}{(PSC+1) \times (ARR+1)} = \frac{32 \times 10^6 \ Hz}{(11+1) \times (45+1)} = 57971 \ Hz \qquad (10)$$

Figure 35. STM32 general-purpose timer diagram [37].

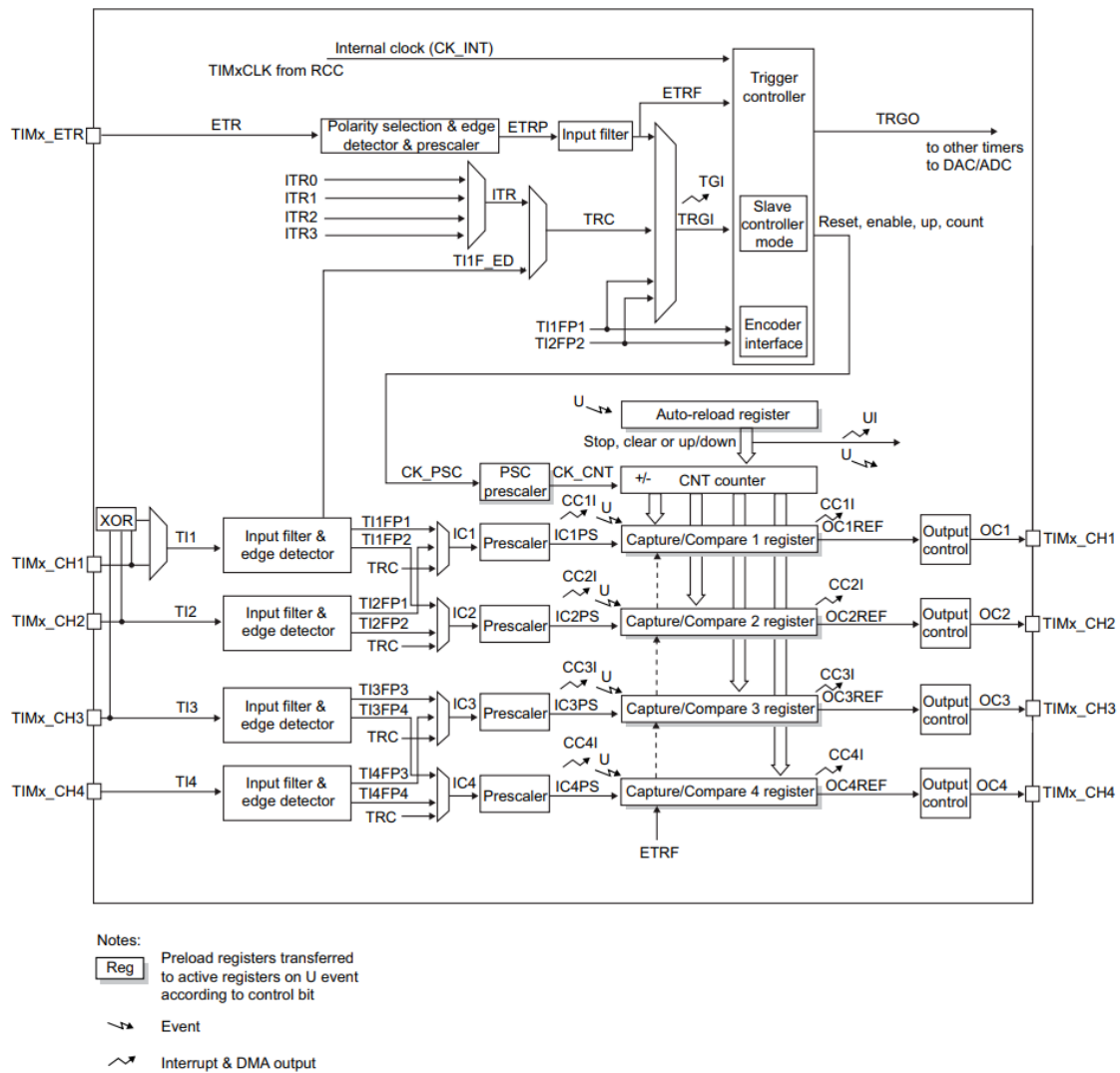To configure the duty cycle of the output, output compare feature is used. That compares the counting CNT value to set CCR (capture/compare register) value and adjusts the output if it is crossed. The behaviour of it is shown in Figure 36. Because a bit of the communication consists of 6 pulses and a UART byte consists of 8 data, 1 start and 1 stop bit, additional logic is needed.
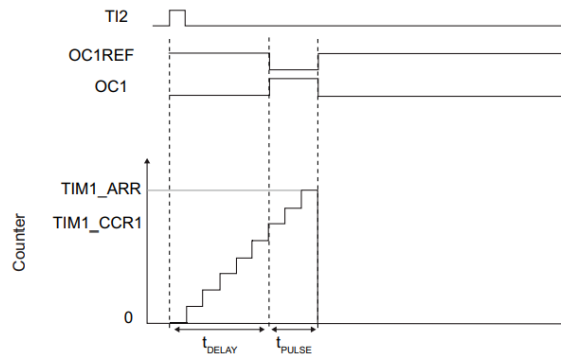

Figure 36. One pulse of PWM (Pulse-Width Modulation) signal generation [37].

At every pulse end, a timer interrupt is generated where state of the code transmission is handled. The implementation of timer interrupt that handles code transmission at needed carrier frequency is presented in Figure 37. The *pulseCnt* indicates how many pulses of last bit have been sent, since 6 pulses are needed per bit. *BitNr* is used to track which bit is currently in transmission. The CCR value that is adjusted is a microcontroller timer register used to change duty cycle of the signal.

The handler starts with the detection of current pulse count. The pulse count is incremented each timer interrupt until the end of bit is reached. If end of bit is reached, the end of code to be transmitted is checked. On the end of code transmission, variables are reinitialized to 0, and timer is turned off. Timer is turned on again in the main loop, according to desired code transmission frequency. At each bit transmission, PWM duty cycle is actively adjusted according to current bit level on the code to be transmitted. Finally, when the byte is sent, the interrupt is cleared.

53

Timer 22 Interrupt Handler

Interrupt Entry

pulseCnt >= 5 ? —Yes→ bitNr < 10 ? —Yes→ if bit number bitNr at code is high? —No→ CCR = 0

No (pulseCnt >= 5?): Increment pulseCnt

No (bitNr < 10?):
CCR = 0
pulseCnt = 0
bitNr = 0
Stop timer

Reinitialize variables, stop timer

Yes (if bit number bitNr at code is high?): Set CCR to duty cycle value

pulseCnt = 0
Increment bitNr
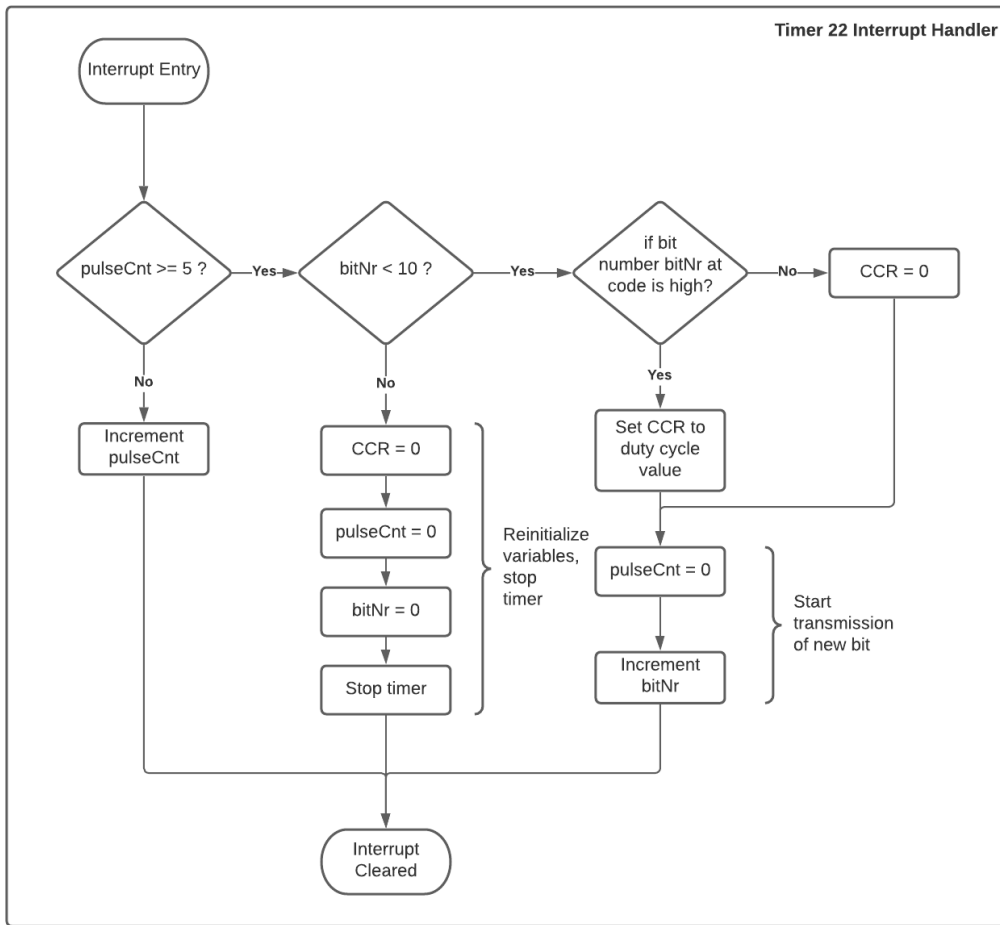
Start transmission of new bit

Interrupt Cleared

Figure 37. Code transmission with carrier frequency interrupt handler.

8 Verification

To verify the targeted accuracy, a verification test was done. The device used to test against is a Seiko S149 with laser-photocell system providing the trigger signal. The device is used by EAL (*Eesti Autospordi Liit*) in Estonian rallys. The device provides up to one-hundredth second lap times (10 ms), but the accuracy itself is not defined [38]. More accurate device is needed for full-extent accuracy testing. However, as a better device was not to be found, comparison was done with this device to provide basic verification.

8.1 Verification setup

The test was done on formula student skid pad track, where total of 4 laps are done by running right and left circle 2 times as shown in Figure 38. As seen in Figure 39, the laser-photocell and the infrared beacon were placed close to each other in the start/stop line to get measurements as close as possible.
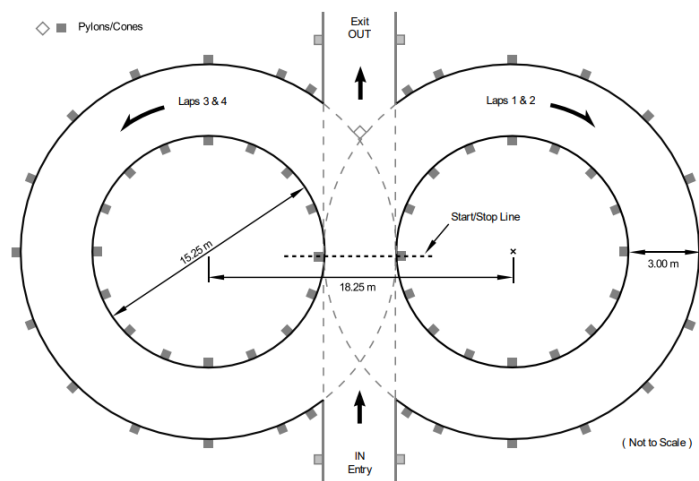

Figure 38. Formula student skid pad course [39].

Figure 39. Placement of device under test and verification device on skid pad start/stop line.

8.2 Verification results

Total of 55 laps were done with duplicated lap time measurements. The results from the Seiko S149 were compared to the lap times shown in GEMS Data Analysis Pro that were triggered by the designed IR receiver system via CAN bus message seen in Figure 40. The beacon ID code that is received from beacon is sent directly to CAN bus, which is used for detection of new lap/split. The program then itself marks the lap detection in time graphs with red dotted line, thus eases analysis of log files.

Figure 40. GEMS Data Analysis Pro screenshot of log file including detected lap times.

The designed beacon results are with 1 ms precision, while the provided verification device provides 10 ms precision. That creates a multimodal distribution of error between the measurement results with peaks near -10 ms, 0 ms and 10 ms presented in histogram format in Figure 41.

The results show that in addition to 10 ms inaccuracy provided by the verification device precision, there is additional error up to 5 ms. This is close to the theoretical error that is shown in Figure 14.
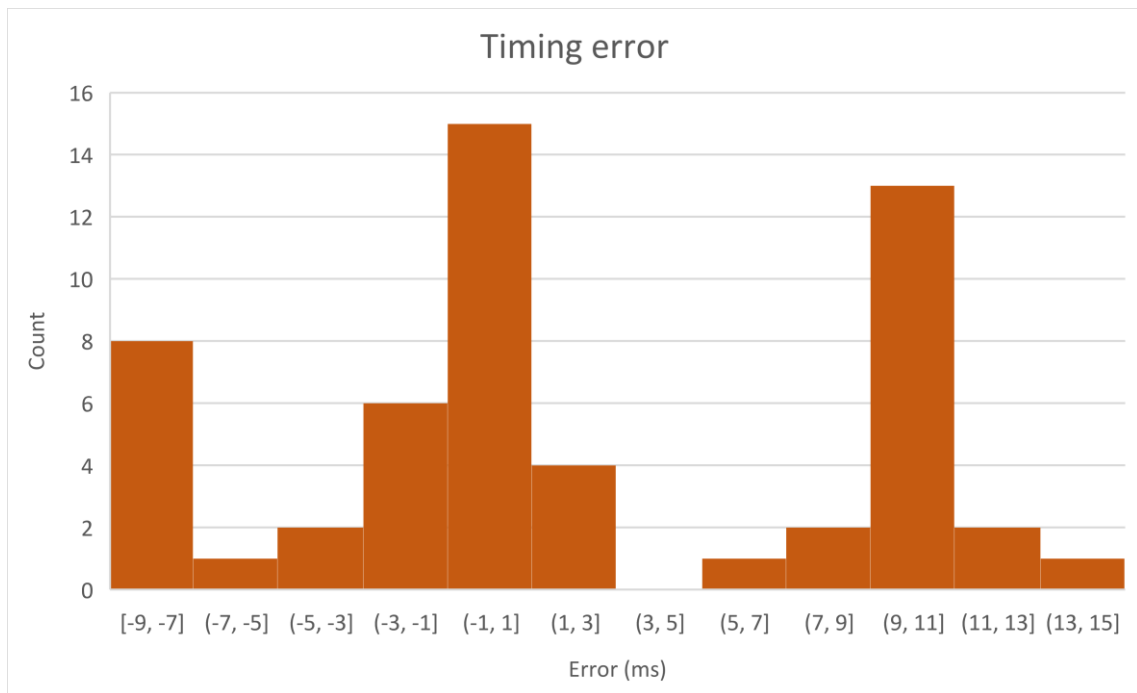

Figure 41. Histogram of lap time measurement error.

57

9 Summary

The goal of the thesis was to develop a lap timing system for formula student car. Firstly, the targets were set for the design regarding functionality, measurement accuracy and runtime on battery in cooperation with FS Team Tallinn. After exploring currently available devices in the market, different design concepts were proposed. The main components and principles were tested as a prototype before any real PCB design was done.

After successful main component testing, the same main components were used in the final design. The electronic circuits and layouts were designed for the beacon and receiver. Software architecture was described and some critical parts analysed in flowchart. Prototype was assembled and tested on formula student car.

Verification could not be done on to full extent due to lack of such device on hand. However basic functionality was verified with less precise device to get general acceptance to be used in future testing. To verify the developed system to full extent, future work shall include finding a suitable verification device and run verification tests once again.

References

[1]   "Formula SAE," Wikipedia, [Online]. Available:
       https://en.wikipedia.org/wiki/Formula_SAE.

[2]   "MoTeC BTX Beacon Transmitter," Race Data Systems, [Online]. Available:
       https://www.racedatasystems.com/products/motec-btx-beacon-transmitter.

[3]   "AIM lap timer," GmbH Memotec, [Online]. Available: https://www.me-mo-
       tec.com/en/Services/General%20information/AIM%20lap%20timer/AiM-lap-
       timer.html.

[4]   "TYPES OF RFID SYSTEMS," Impinj, [Online]. Available:
       https://www.impinj.com/about-rfid/types-of-rfid-systems/.

[5]   "PR1a Photocell and Variations," ALGE-TIMING, [Online]. Available:
       https://alge-timing.com/AlgeTiming_V2/en/impulse-devices/pr1a.html#tab0:tab-
       schematics-2415.

[6]   M. Niggel, "Lap Timing Guide for Drone Racing," Propwashed, [Online].
       Available: https://www.propwashed.com/lap-timing-guide-drone-racing/.

[7]   "MoTeC BTX Beacon Transmitter," Race Data Systems, [Online]. Available:
       https://www.racedatasystems.com/products/motec-btx-beacon-transmitter.

[8]   "Aim IR Lap Timing Transmitter," Integrated Motorsport Solutions, [Online].
       Available: https://www.integrated-motorsport.com/collections/gps-lap-
       timing/products/aim-ir-lap-timing-transmitter.

[9]   "Stack Lap Time System Beacon," Demon Tweeks, [Online]. Available:
       https://www.demon-tweeks.com/eu/stack-lap-timing-beacon-stast544/.

[10]   "LTI Hot Lap Timer," Hoerr Racing Products, [Online]. Available:
       https://www.hrpworld.com/la21710-longacre-hot-lap-system.html.

[11]   "WIRELESS PHOTOCELL HL3-131," Sports Timing Systems, [Online].
       Available: https://www.sportstimingsystems.co.uk/shop/photocell-
       solutions/photocells/wireless-photocell-hl3-131.html.

[12]   "Cronox 2.0," Cronox, [Online]. Available: https://cronox-
       sports.com/shop/cronox-2-0/.

[13]   "Racelogic VBOX LapTimer," DEMON TWEEKS, [Online]. Available:
       https://www.demon-tweeks.com/eu/racelogic-vbox-laptimer-rlgrlvblap01/.

[14]   "Qstarz LT-Q6000 GPS laptimer Zwart," Conrad, [Online]. Available:
       https://www.conrad.nl/p/qstarz-lt-q6000-gps-laptimer-zwart-374206.

[15]   "IDEC (DECODER) - 1-PORT," Westhold Corporation, [Online]. Available:
       https://shop.westhold.com/idec-decoder-1-port/.

[16]   "IRLED SELECTION GUIDE FOR Si114X PROXIMITY APPLICATIONS,"
       Silicon Labs, [Online]. Available:
       https://www.silabs.com/documents/public/application-notes/AN521.pdf.

[17]   "Steradian," Wikipedia, [Online]. Available:
       https://en.wikipedia.org/wiki/Steradian.

[18]   D. K. Borah, C. C. Davis, A. Boucouvalas, S. Hranilovic and K. Yiannopoulos,
       "A review of communication-oriented optical wireless systems," ResearchGate,
       2012.

[19] R. Marston, "SECURITY ELECTRONICS SYSTEMS AND CIRCUITS — PART 5," NUTS & VOLTS MAGAZINE, 1998. [Online]. Available: https://www.nutsvolts.com/magazine/article/security-electronics-systems-and-circuits-part-5.

[20] "IR Receiver Modules for Data Transmission - TSDP341," Vishay Semiconductors, [Online]. Available: https://www.vishay.com/docs/82667/tsdp341.pdf.

[21] "Vishay's TSDP Receiver Series for Infrared Data Communications," Vishay Semiconductors, [Online]. Available: https://www.vishay.com/docs/82666/tsdpreceiver.pdf.

[22] "Circuit Description of the IR Receiver Modules," Vishay Semiconductors, [Online]. Available: https://www.vishay.com/docs/80069/circuit.pdf.

[23] "IR Receiver Modules for Remote Control Systems - TSOP48," Vishay Semiconductors, [Online]. Available: https://www.vishay.com/docs/82459/tsop48.pdf.

[24] "Bus Arbitration And Message Identification," Embedclogic, [Online]. Available: https://embedclogic.com/can-protocol-protocol-to-broadcast-message-on-a-network/can-bus-arbitration-and-message-identification/.

[25] "CAN data link layers in some detail," CAN in Automation, [Online]. Available: https://www.can-cia.org/can-knowledge/can/can-data-link-layers/.

[26] J. Howie, "Multi-Sheet and Multi-Channel Design," Altium Limited, [Online]. Available: https://www.altium.com/documentation/altium-designer/multi-sheet-and-multi-channel-design-ad?version=18.1#!hierarchical-design.

[27] "MOSFET Gate Drive Circuit," Toshiba, [Online]. Available: https://toshiba.semicon-storage.com/info/docget.jsp?did=13415.

[28] "IRLML6346TRPbF," International Rectifier, [Online]. Available: https://www.infineon.com/dgdl/irlml6346pbf.pdf?fileId=5546d462533600a401535668a336262e.

[29] "STM32 32-bit Arm Cortex MCUs," STMicroelectronics, [Online]. Available: https://www.st.com/en/microcontrollers-microprocessors/stm32-32-bit-arm-cortex-mcus.html.

[30] "BU-1006: Cost of Mobile and Renewable Power," Battery University, 2021. [Online]. Available: https://batteryuniversity.com/index.php/learn/article/bu_1006_cost_of_mobile_power.

[31] "LMR50410 SIMPLE SWITCHER® 4-V to 36-V, 1-A Buck Converter in SOT-23-6 Package," Texas Instruments, [Online]. Available: https://www.ti.com/lit/ds/symlink/lmr50410.pdf?ts=1615555530595.

[32] "Datasheet - STM32F730x8," STMicroelectronics, [Online]. Available: https://www.st.com/resource/en/datasheet/stm32f730r8.pdf.

[33] "Signal and Power Isolated CAN Transceiver," Analog Devices, [Online]. Available: https://eu.mouser.com/datasheet/2/609/ADM3053-1503195.pdf.

[34] S. Corrigan, "Common-mode effects in CAN networks," Kvaser, [Online]. Available: https://can-newsletter.org/uploads/media/raw/c190a7e99e71c41e1bf4692d5da58cd1.pdf.

[35] "Description of STM32F4 HAL and low-layer drivers," STMicroelectronics, [Online]. Available: https://www.st.com/resource/en/user_manual/dm00105879-description-of-stm32f4-hal-and-lowlayer-drivers-stmicroelectronics.pdf.

[36] "STM32 Embedded Software," STMicroelectronics, [Online]. Available: https://www.st.com/content/ccc/resource/sales_and_marketing/presentation/produ ct_presentation/37/55/ff/bc/a8/71/4f/c5/stm32_embedded_software_offering.pdf/f iles/stm32_embedded_software_offering.pdf/jcr:content/translations/en.stm32_e mbedded_software_offer.

[37] "Ultra-low-power STM32L0x3 advanced Arm®-based 32-bit MCUs," STMicroelectronics, [Online]. Available: https://www.st.com/resource/en/reference_manual/dm00095744-ultralowpower-stm32l0x3-advanced-armbased-32bit-mcus-stmicroelectronics.pdf.

[38] "SEIKO S149 Instruction," Seiko, [Online]. Available: https://storage.seikowatches.com/production/files/2018/03/20/143357142614/pdf/ SEIKO_S149.pdf.

[39] F. SAE, "Formula SAE Rules 2021 Version 1.0," [Online]. Available: https://www.fsaeonline.com/cdsweb/gen/DownloadDocument.aspx?DocumentID =6d9f4b51-a642-425c-bfdf-5f95b4e5e10b.

Appendix 1 – Non-exclusive licence for reproduction and publication of a graduation thesis[1]

I Mario Stepanov

1. Grant Tallinn University of Technology free licence (non-exclusive licence) for my thesis "Lap Timing System for Formula Student Car FEST21", supervised by Olev Märtens

    1.1. to be reproduced for the purposes of preservation and electronic publication of the graduation thesis, incl. to be entered in the digital collection of the library of Tallinn University of Technology until expiry of the term of copyright;

    1.2. to be published via the web of Tallinn University of Technology, incl. to be entered in the digital collection of the library of Tallinn University of Technology until expiry of the term of copyright.

2. I am aware that the author also retains the rights specified in clause 1 of the non-exclusive licence.

3. I confirm that granting the non-exclusive licence does not infringe other persons' intellectual property rights, the rights arising from the Personal Data Protection Act or rights arising from other legislation.

09.05.2021

---

1 The non-exclusive licence is not valid during the validity of access restriction indicated in the student's application for restriction on access to the graduation thesis that has been signed by the school's dean, except in case of the university's right to reproduce the thesis for preservation purposes only. If a graduation thesis is based on the joint creative activity of two or more persons and the co-author(s) has/have not granted, by the set deadline, the student defending his/her graduation thesis consent to reproduce and publish the graduation thesis in compliance with clauses 1.1 and 1.2 of the non-exclusive licence, the non-exclusive license shall not be valid for the period.